

Czech Technical University in Prague  
Faculty of Nuclear Sciences and Physical Engineering

## **HABILITATION THESIS**

### **Spectral Theory Problems on Graphs and Their Applications**

(version without appendices)

Prague 2022

Jiří Lipovský

To my wife Veronika.

I would like to thank all co-authors of the papers in the attachment of this thesis, namely prof. Pavel Exner, prof. Pedro Freitas, prof. Leszek Sirko, dr. hab. Michał Ławniczak and dr. Małgorzata Białous, for their contribution to these joint works. I am very much obliged to my wife Veronika and to my parents for their support during my scientific career.

I acknowledge the support of the Czech Science Foundation grants 15-14180Y, 17-01706S, 18-00496S, and 22-18739S, OP RDE project “International mobilities for research activities of the University of Hradec Králové” CZ.02.2.69/0.0/0.0/16\_027/0008487, and FCT (Portugal) grant PTDC/MAT-CAL/4334/2014. I am also indebted to my employer, the University of Hradec Králové and its internal projects, and to the University of Lisbon for its hospitality during my stay in Lisbon in the years 2018-19.

I declare that I carried out this habilitation thesis independently, and only with the cited sources, literature, and other professional sources.

In Hradec Králové, August 26th, 2022

# Bibliografický záznam

Autor	Jiří Lipovský
Název habilitační práce	Problémy ze spektrální teorie na grafech a jejich aplikace
Obor	Aplikovaná matematika
Afiliace autora	Univerzita Hradec Králové, Přírodovědecká fakulta, Katedra fyziky
Habilitační řízení vedeno na	České vysoké učení technické v Praze, Fakulta jaderná a fyzikálně inženýrská
Rok	2022
Počet stran	vii+216
Klíčová slova	spektrální teorie, kvantové grafy, mikrovlnné grafy, vlnová rovnice s tlumením, spektrální determinant

## Bibliographic entry

Author	Jiří Lipovský
Title of Habilitation Thesis	Spectral Theory Problems on Graphs and Their Applications
Field	Applied Mathematics
Affiliation of the Author	University of Hradec Králové, Faculty of Science, Department of Physics
Habilitation at	Czech Technical University in Prague, Faculty of Nuclear Sciences and Physical Engineering
Year	2022
Number of Pages	vii+216
Keywords	spectral theory, quantum graphs, microwave graphs, damped wave equation, spectral determinant

# Abstrakt

Předkládaná habilitační práce je souborem devíti článků ze spektrální teorie. Bylo použito několik modelů, konkrétně kvantové grafy, mikrovlnné sítě, vlnová rovnice s tlumením a polyharmonický operátor. Operátory použité v práci působí na metrických grafech, a to jak kompaktních, tak otevřených. Získali jsme spektrální vlastnosti kvantových grafů s vazebnou podmínkou preferované orientace, našli jsme Gelfandovu-Levitanovu trace formuli pro kvantový graf s generickými vazebnými podmínkami a studovali rezonanční vlastnosti otevřených kvantových grafů. Výsledky pro kvantové grafy byly ověřeny ve dvou článcích o experimentech s mikrovlnnými sítěmi. Studovali jsme asymptotické spektrální vlastnosti vlnové rovnice s tlumením na grafech a spektrální determinant pro polyharmonický operátor.

# Abstract

The present habilitation thesis is a collection of nine papers in spectral theory. Several models are used, namely, quantum graphs, microwave networks, damped wave equation, and the polyharmonic operator. The operators used in the thesis act on metric graphs; both compact and open graphs are used. Spectral properties of quantum graphs with preferred-orientation coupling are obtained, the Gelfand-Levitan trace formula is found for quantum graphs with generic coupling conditions, and resonance properties of open quantum graphs are investigated. The results on quantum graphs are verified in two papers on microwave networks' experiments. Asymptotic spectral properties of the damped wave equation on graphs and the spectral determinant for the polyharmonic operator are investigated.

# Contents

<b>1</b>	<b>Introduction</b>	<b>3</b>
<b>2</b>	<b>Quantum Graphs</b>	<b>5</b>
2.1	Description of the Model . . . . .	5
2.2	Examples of the Coupling Conditions . . . . .	8
2.3	Gelfand-Levitan Trace Formula . . . . .	11
2.4	Resolvent and Scattering Resonances . . . . .	12
2.5	Weyl Asymptotics . . . . .	14
2.6	Pseudo-Orbit Expansion for the Graphs with External Edges . . . . .	15
2.7	Fermi Golden Rule . . . . .	18
2.8	Results on Quantum Graphs . . . . .	19
2.8.1	Spectral Asymptotics of the Laplacian on Platonic Solids Graphs . . . . .	20
2.8.2	Topological Bulk-Edge Effects in Quantum Graph Transport	21
2.8.3	A Gelfand-Levitan Trace Formula for Generic Quantum Graphs . . . . .	23
2.8.4	Pseudo-Orbit Approach to Trajectories of Resonances in Quantum Graphs with General Vertex Coupling: Fermi Rule and High-Energy Asymptotics . . . . .	24
2.8.5	On the Effective Size of a Non-Weyl Graph . . . . .	25
<b>3</b>	<b>Microwave Graphs</b>	<b>27</b>
3.1	Description of the Model and Setup . . . . .	27
3.2	Results on Microwave Graphs . . . . .	28
3.2.1	Non-Weyl Microwave Graphs . . . . .	28
3.2.2	Application of Topological Resonances in Experimental In- vestigation of a Fermi Golden Rule in Microwave Networks	30
<b>4</b>	<b>Damped Wave Equation</b>	<b>31</b>
4.1	Results on the Damped Wave Equation . . . . .	32
4.1.1	Eigenvalue Asymptotics for the Damped Wave Equation on Metric Graphs . . . . .	32
<b>5</b>	<b>Polyharmonic Operator</b>	<b>34</b>
5.1	Spectral Determinant . . . . .	34



*CONTENTS*

---

5.2 Results on the Polyharmonic Operator . . . . .	35
5.2.1 The Determinant of One-Dimensional Polyharmonic Operators of Arbitrary Order . . . . .	35
<b>Bibliography</b>	<b>37</b>
<b>List of Notation</b>	<b>44</b>
<b>Attachments</b>	<b>46</b>
<b>A Spectral Asymptotics of the Laplacian on Platonic Solids Graphs</b>	<b>47</b>
<b>B Topological Bulk-Edge Effects in Quantum Graph Transport</b>	<b>48</b>
<b>C A Gelfand-Levitan Trace Formula for Generic Quantum Graphs</b>	<b>49</b>
<b>D Pseudo-Orbit Approach to Trajectories of Resonances in Quantum Graphs with General Vertex Coupling: Fermi Rule and High-Energy Asymptotics</b>	<b>50</b>
<b>E On the Effective Size of a Non-Weyl Graph</b>	<b>51</b>
<b>F Non-Weyl Microwave Graphs</b>	<b>52</b>
<b>G Application of Topological Resonances in Experimental Investigation of a Fermi Golden Rule in Microwave Networks</b>	<b>53</b>
<b>H Eigenvalue Asymptotics for the Damped Wave Equation on Metric Graphs</b>	<b>54</b>
<b>I The Determinant of One-Dimensional Polyharmonic Operators of Arbitrary Order</b>	<b>55</b>

# Chapter 1

## Introduction

Many problems in physics can be described by the properties of various operators. The tools of the spectral theory allow us to use a precise mathematical description of the employed models. The properly defined notions appear in the theorems that exactly describe the properties of the system. The obtained results can be then measured in an experiment and can have possible applications in the future.

While describing a physical phenomenon, one can choose either a simple one-dimensional model or try to describe the phenomenon in higher dimensions which allows covering nontrivial effects with the cost of a more complicated model. Choosing a metric graph as the “playground” for the model joints the advantages of both options: the simplicity of a one-dimensional model and the complexity of a non-trivial topological structure.

The present thesis is a collection of nine papers by the author in spectral theory and its applications. They cover various models in physics while the “red thread” tying them together is a metric graph. The first five papers describe the behaviour of a quantum particle on the graph. The particle may not only interact with the electric potential which appears in the Gelfand-Levitan trace formula in Appendix C, but its behaviour can also be influenced by the coupling conditions at the vertices of the graph. The preferred-orientation coupling used in Appendices A and B breaks the time invariance of the model and has interesting asymptotic properties that differ for odd and even vertex degrees. The properties of the resonances for open quantum graphs are investigated in Appendices D and E. The quantum graphs, studied in the first five papers, have similar properties to microwave graphs. This equivalence of the two equations allows us to experimentally verify the results obtained for quantum graphs using a microwave network, as shown in publications in Appendices F and G. These two papers illustrate that the spectral theory problems are not only neat mathematical exercises but can be measured in a real physical system. The paper in Appendix H studies the damped wave equation on a metric graph and its spectral properties. One of the possible applications of the damped wave equation can be the description of spider webs. Finally, the last model is the polyharmonic operator, for which the spectral determinant was studied in Appendix I; in this case, we used the simple

graph – an interval.

In the next four chapters, the models of quantum graphs, microwave graphs, the damped wave equation, and the polyharmonic operator are described. Necessary notions needed for stating the main results of the papers are defined and briefly explained. At the end of each chapter, the main results of the attached papers are given. The bibliography is followed by the list of the symbols used in the main part of the thesis.

The contribution of the author of the habilitation thesis was following. In papers in Appendices A–D, and H–I the author performed the computations, after consultations with the co-author he obtained the results and wrote the first draft. The author also performed the numerical calculations in Appendices B and H. In the works in Appendices F and G the author suggested performing the experiment, collaborated on the proposition of the structure of the microwave networks, wrote the theoretical part of the paper, and collaborated on the introductions of the papers, and partly collaborated on the numerics. J.L. is the only author of the paper in Appendix E.

# Chapter 2

## Quantum Graphs

Quantum graphs are a rather simple model which enables the description of the behaviour of a quantum particle on a network. From the mathematical point of view, they are a set of ordinary differential equations coupled with the matching conditions at the vertices of the graph.

The beginnings of this model can be traced back to the 1930s when L. Pauling used it to describe the diamagnetic properties of benzene and other aromatic molecules [Pau36]. Later K. Ruedenberg and C.W. Scherr [RS53] applied the model for treating electrons in the aromatic molecules. They assumed that  $\sigma$ -electrons form bonds maintaining the molecular frame and described the notion of the  $\pi$ -electrons in this frame using the first approximation of the one-dimensional model. Quantum graphs became more popular in the 1980s.

Quantum graphs aim to describe various mesoscopic structures. They are a simplification for so-called *quantum wires*; in quantum graphs, however, the width of the wires is assumed to be small compared to its length. A more general model, a quantum waveguide, describes the behaviour of a quantum particle in a waveguide with non-zero width. For various results in this area, we refer the reader to the monograph [EK15]. From the mathematical point of view, these problems are PDEs. The same holds true if we study a network created from these waveguides, the so-called *fattened graphs*. There are various results stating that Laplacians on the fattened graphs converge to Laplacians on quantum graphs when the width of the waveguides shrinks, see [Pos12] and references therein. Another example of generalization of quantum graphs are *leaky graphs* [Exn07], which allow the particle to tunnel through the edges. Due to its simplicity, the model of quantum graphs is also used as a toy model, for instance for the description of quantum chaos (see, e.g. [KS00, BK13, KS97, BBK01]).

### 2.1 Description of the Model

Let us assume a metric graph  $\Gamma$  consisting of the set of  $\tilde{V}$  vertices  $\mathcal{V} = \{\mathcal{X}_j\}_{j=1}^{\tilde{V}}$ , the set  $\mathcal{E}_I = \{e_j\}_{j=1}^N$  of  $N$  finite edges characterized by their length  $\ell_j$  and the set  $\mathcal{E}_E = \{e_j\}_{j=N+1}^{N+M}$  of  $M$  external edges of infinite length. The internal edges

connect two vertices and therefore can be parametrized by the intervals  $(0, \ell_j)$ . The external edges can be represented by half-lines with the starting point being one of the vertices; they are usually parametrized by the intervals  $(0, \infty)$ . The degree (the number of edges emanating from the vertex) of the vertex  $\mathcal{X}_j$  is denoted by  $d_j$ . The Hilbert space of the whole system is

$$\mathcal{H} = \bigoplus_{i=1}^N L^2((0, \ell_i)) \oplus \bigoplus_{i=1}^M L^2((0, \infty)).$$

The states in this Hilbert space can be represented by the vectors

$$\psi = (\psi_1, \dots, \psi_N, \psi_{N+1}, \dots, \psi_{N+M})^T.$$

The structure of the metric graph is equipped with the second order differential operator  $H$  acting as

$$-\frac{d^2}{dx^2} + q(x), \quad (2.1)$$

where the (electric) potential  $q(x)$  is a bounded function supported on the internal edges of the graph. In some works, the magnetic potential is used as well; however, we will not introduce it in the present thesis. The above-defined operator is the Hamiltonian of a quantum particle in one dimension considered in a certain set of units. For simplicity, the factor  $\frac{\hbar^2}{2m}$  is dropped, which can be explained by choosing the set of units in which, for instance,  $\hbar = 1$  and  $m = \frac{1}{2}$ . In most of the papers in the appendices, the potential is considered to be zero and instead of the above-defined Schrödinger operator the Laplacian is considered.

The domain of the operator consists of functions in the Sobolev space  $W^{2,2}(\Gamma)$  (for definitions of the Sobolev spaces in a more general setting we refer the reader to [Eva98]) satisfying the coupling conditions. We should stress that by  $W^{2,2}(\Gamma)$  we mean the orthogonal sum of the Sobolev spaces  $W^{2,2}(e_j)$ . In other words, the edge components of the wavefunction are in the appropriate Sobolev space but the function is allowed to be discontinuous at the vertices of the graph. The coupling conditions (sometimes called matching or boundary conditions) at the vertex  $\mathcal{X}_j$  which define the general self-adjoint operator can be written in the form

$$(U_j - I)\Psi_j + i(U_j + I)\Psi'_j = 0, \quad (2.2)$$

where  $U_j$  is a unitary  $d_j \times d_j$  matrix,  $I$  denotes the  $d_j \times d_j$  identity matrix, the column vectors  $\Psi_j$  and  $\Psi'_j$  are the vectors of function values and outward derivatives at the vertex, respectively. We stress that the derivative in the coupling conditions should be taken outward, i.e., with the positive sign if it corresponds to  $x = 0$  and the negative sign for  $x = \ell_j$ . The general coupling condition for a self-adjoint quantum graph was independently obtained by V. Kostrykin and R. Schrader [KS99a] and M. Harmer [Har00].

Hence the triplet  $\{\Gamma, q(x), \{U_j\}_{j=1}^{\tilde{V}}\}$  consisting of the metric graph (including the knowledge of the lengths of the edges and the topology of the graph), the

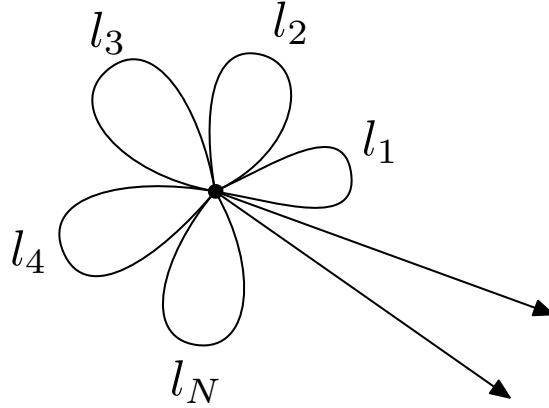


Figure 2.1: A flower-like graph. Reproduced from [EL10].

potential (on the whole graph, i.e. consisting of the edge components) and the set of unitary coupling matrices describes the quantum graph. However, there is a way to replace the unitary coupling matrices for particular vertices with a big  $(2N + M) \times (2N + M)$  unitary matrix describing the coupling on the whole graph and also the topology of the graph. The idea of this construction is to introduce a one-vertex “flower-like” model, which first appeared in [Kuc08] and was later used in e.g. [EL10], see Figure 2.1.

The coupling condition considered in this model is

$$(U - I)\Psi + i(U + I)\Psi' = 0, \quad (2.3)$$

where the  $(2N + M) \times (2N + M)$  unitary matrix  $U$  can be by a similarity transformation mapped to a block diagonal matrix with blocks  $U_j$ . The vectors

$$\begin{aligned} \Psi &= (f_1(0), f_1(\ell_1), f_2(0), f_2(\ell_2), \dots, f_N(0), f_N(\ell_N), g_1(0), g_2(0), \dots, g_M(0))^T, \\ \Psi' &= (f'_1(0), -f'_1(\ell_1), f'_2(0), -f'_2(\ell_2), \dots, f'_N(0), -f'_N(\ell_N), g'_1(0), g'_2(0), \dots, g'_M(0))^T, \end{aligned}$$

of lengths  $(2N + M)$  are the vectors of function values and outward derivatives. In the above expressions,  $f_j(x)$  denotes the wavefunction component at the internal edge  $e_j$  and  $g_j(x)$  the wavefunction component at the external edge  $e_{N+j}$ .

Note that an alternative form of the coupling condition (2.3) can be used: the term with  $U + I$  can be multiplied by a real parameter  $\ell$  [FT00].

$$(U - I)\Psi + i\ell(U + I)\Psi' = 0. \quad (2.4)$$

However, this coupling condition (2.4) is equivalent to the equation (2.3) since to each  $\ell$  and  $U$  there exist a unitary matrix  $U_\ell$  such that (2.3) with the coupling matrix  $U_\ell$  gives the same condition as (2.4). There are also different descriptions of the coupling conditions on the graph. One can use square matrices  $A_j, B_j$  instead of  $U - I$  and  $i(U + I)$  that satisfy the condition that  $A_j B_j^*$  is self-adjoint and the joint matrix  $(A_j, B_j)$  has maximal rank [KS99a]. Another option is to use

the projector to the Dirichlet part (the eigenspace of  $U$  for the eigenvalue  $-1$ ), the projector to the Neumann part (the eigenspace of  $U$  for the eigenvalue  $1$ ) and, finally, the projector to the Robin part. Moreover, the matrices  $A_j$  and  $B_j$  can be chosen in a particular form with certain blocks equal to zero, as suggested in [CET10]. All these formulations of the coupling condition are equivalent to each other and they define a self-adjoint operator (see, e.g. [BK13, Lip16b]).

## 2.2 Examples of the Coupling Conditions

In this section, we introduce some of the most common coupling conditions.

### 1. Permutation Symmetric Coupling

This coupling is symmetric with respect to exchanging any two edges emanating from the vertex. The coupling matrix can be written in the form  $U = aJ + bI$ , where  $I$  is the identity matrix,  $J$  is the matrix with all entries equal to one, and  $a$  and  $b$  are complex constants. The coupling matrix  $U$  is unitary iff  $|b|^2 = 1$  and  $|d_j a + b| = 1$ .

### 2. $\delta$ -coupling

This coupling is a particular case of the permutation symmetric coupling. The unitary coupling matrix is  $U = \frac{2}{d_j + i\alpha} J - I$ , where  $i$  is the complex unit and  $\alpha$  is the real parameter.  $\alpha$  is called the *strength* of the coupling. In the case of a vertex of degree 2, it corresponds to the singular potential equal to the  $\alpha$ -multiple of the  $\delta$ -distribution. The coupling condition (2.3) at a vertex  $\mathcal{X}$  can be written as

$$\begin{aligned} f(\mathcal{X}) := f_i(\mathcal{X}) &= f_j(\mathcal{X}) \quad \text{for all } i, j \text{ such that } \mathcal{X} \in e_i \cap e_j, \\ \sum_{j: \mathcal{X} \in e_j} f'_j(\mathcal{X}) &= \alpha f(\mathcal{X}). \end{aligned}$$

The function is continuous at the vertex and the sum of the outward derivatives is equal to  $\alpha$ -multiple of this function value.

### 3. $\delta'_s$ -coupling

Another particular case of the permutation-symmetric coupling is the symmetric  $\delta'$ -condition. It is a counterpart of the  $\delta$ -condition and, in contrast to this condition, the role of the function values and derivatives is exchanged. However, the name  $\delta'$  is not very fortunate; the coupling does **not** correspond to the derivative of the  $\delta$ -distribution potential. The condition at the vertex  $\mathcal{X}$  can be written as

$$\begin{aligned} f'(\mathcal{X}) := f'_i(\mathcal{X}) &= f'_j(\mathcal{X}) \quad \text{for all } i, j \text{ such that } \mathcal{X} \in e_i \cap e_j, \\ \sum_{j: \mathcal{X} \in e_j} f_j(\mathcal{X}) &= \beta f'(\mathcal{X}). \end{aligned}$$

Here,  $\beta$  is a real parameter, it is called, as in the  $\delta$ -condition case, the *strength* of the coupling. Outward derivatives are equal to each other and the sum of the function values is equal to a  $\beta$ -multiple of this derivative. The unitary coupling matrix is  $U = I - \frac{2}{d_j - i\beta} J$ .

4.  **$\delta'$ -coupling**

The  $\delta'$ -condition can be generalized from the vertex of degree 2 to the vertex of general degree  $d_j$  also in this, slightly different formulation. The condition is

$$\begin{aligned} f_i(\mathcal{X}) - f_j(\mathcal{X}) &= \frac{\beta}{d_j} (f'_i(\mathcal{X}) - f'_j(\mathcal{X})) \quad \text{for all } i, j \text{ such that } \mathcal{X} \in e_i \cap e_j, \\ \sum_{j: \mathcal{X} \in e_j} f'_j(\mathcal{X}) &= 0. \end{aligned}$$

and corresponds to the coupling matrix  $U = \frac{2}{d_j - i\beta} J - \frac{d_j + i\beta}{d_j - i\beta} I$ .

5. **Standard Coupling** (known also as Kirchhoff, free or Neumann-Kirchoff)

This is the particular case of  $\delta$ -coupling for the coupling strength going to zero,  $\alpha = 0$ . This coupling is the most physical one, it corresponds to the situation when the particle freely moves through the vertex. Although several names are used for this condition, in this text, we prefer the name “standard”. The name “Kirchhoff” is not very fortunate, as all the self-adjoint conditions satisfy the probability current conservation. The conditions are

$$\begin{aligned} f(\mathcal{X}) := f_i(\mathcal{X}) &= f_j(\mathcal{X}) \quad \text{for all } i, j \text{ such that } \mathcal{X} \in e_i \cap e_j, \\ \sum_{j: \mathcal{X} \in e_j} f'_j(\mathcal{X}) &= 0. \end{aligned}$$

The unitary matrix is  $U = \frac{2}{d_j} J - I$ .

6. **Dirichlet Coupling Conditions**

These conditions fully separate all the edges connected at the vertex  $\mathcal{X}$  demanding that the function values vanish at the vertex.

$$f_i(\mathcal{X}) = 0 \quad \text{for all } i \text{ such that } \mathcal{X} \in e_i.$$

The unitary matrix is  $U = -I$ .

7. **Neumann Coupling Conditions**

For the Neumann coupling conditions, the vertex is fully decoupled as well. Now we assume that the derivative from each edge vanishes at the vertex  $\mathcal{X}$ .

$$f'_i(\mathcal{X}) = 0 \quad \text{for all } i \text{ such that } \mathcal{X} \in e_i.$$

The unitary matrix is  $U = I$ .



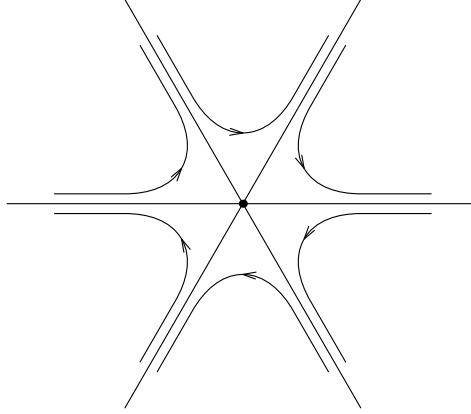


Figure 2.2: Illustration of waves transmitted through the vertex for the preferred-orientation coupling and the energy  $E = 1$ .

### 8. Preferred-Orientation Coupling

This particular coupling, suggested in [ET18] to describe the anomalous quantum Hall effect, is an example of a coupling that does not belong to the set of permutation symmetric couplings. On the other hand, a particular orientation is preferred and the coupling violates the time-reversal invariance. The preferred-orientation coupling is defined by the unitary coupling matrix

$$U = \begin{pmatrix} 0 & 1 & 0 & \dots & 0 \\ 0 & 0 & 1 & \dots & 0 \\ \vdots & \vdots & \vdots & \ddots & \vdots \\ 0 & 0 & 0 & \dots & 1 \\ 1 & 0 & 0 & \dots & 0 \end{pmatrix}.$$

For a particular energy  $E = 1$ , the wave coming from one of the edges is fully transmitted to the neighbouring edge, without loss of generality lying next to it in the clockwise direction. For the other edges, the behaviour of the wave is similar, as Figure 2.2 illustrates. This allowed modeling the anomalous quantum Hall effect for particular types of lattices in [ET18].

For a particle with a general value of energy, this behaviour does not hold anymore. However, the coupling has other interesting properties. In particular, the vertex transparency depends on the parity of the vertex degree. For vertices of odd degree, the scattering matrix asymptotically for large energies behaves as the scattering matrix for the vertex with Neumann coupling. Hence the wave can hardly get through the vertex and is for large energies almost fully reflected. On the other hand, the behaviour of an even-degree vertex is different – as it was shown in [ET18], the reflection and transmission to any edge have similar probabilities for high energies. This difference between the vertex parities follows from the fact that only an even-degree coupling matrix has eigenvalue  $-1$  and hence the Dirichlet

part of the coupling is present. The general proof that the scattering matrix for the vertex without the Dirichlet part of the coupling converges to the one for Neumann coupling, can be found in [KS18].

## 2.3 Gelfand-Levitan Trace Formula

The asymptotic behaviour of the eigenvalues of the given operator can be of interest. There are several types of the so-called trace formulæ in which the spectrum of the operator plays an important role. The first attempts of stating the trace formula for a quantum graph can be traced back to J.-P. Roth [Rot83] and T. Kottos and U. Smilansky [KS99b]. A formula involving integrals of the potential and the eigenfunctions was obtained by R. Carlson in [Car12].

The paper [FL21] in Appendix C deals with the Gelfand-Levitan trace formula, first stated by I.M. Gel'fand and B. Levitan [GL53] for the Schrödinger operator on an interval  $(0, \pi)$  with Neumann boundary conditions. For the Schrödinger operator given by the expression (2.1) under the assumption that the average of the potential is zero they proved that the following formula for the eigenvalues  $\lambda_n(q)$  holds

$$\sum_{n=1}^{\infty} [\lambda_n(q) - \lambda_n(0)] = \frac{1}{4}[q(\pi) + q(0)]. \quad (2.5)$$

The formula can be easily rewritten for the general potential  $q(x)$  for which the condition that its average vanishes is dropped. Let us, for such a potential, define  $\tilde{q}(x) = q(x) - \bar{q}$ , where  $\bar{q} = \frac{1}{\pi} \int_0^\pi q(x) dx$  is the average. The general potential  $q$  satisfies the Schrödinger equation

$$-u_n''(x) + q(x)u_n(x) = \lambda_n(q)u_n(x),$$

where  $\lambda_n$  are the eigenvalues of the Schrödinger operator with  $q$  and  $u_n$  the corresponding eigenfunctions. Subtracting  $\bar{q}u_n(x)$  from both sides of the equation we obtain

$$-u_n''(x) + \tilde{q}(x)u_n(x) = (\lambda_n(q) - \bar{q})u_n(x). \quad (2.6)$$

Hence  $\lambda_n(q) - \bar{q}$  are the eigenvalues for the Schrödinger operator with the potential  $\tilde{q}$ . Moreover, we have

$$\frac{1}{4}[\tilde{q}(\pi) + \tilde{q}(0)] = \frac{1}{4}[q(\pi) - \bar{q} + q(0) - \bar{q}] = \frac{1}{4}[q(\pi) + q(0)] - \frac{1}{2}\bar{q}. \quad (2.7)$$

Substituting (2.7) and the eigenvalues of (2.6) into (2.5) we obtain

$$\sum_{n=1}^{\infty} \left[ \lambda_n(q) - \lambda_n(0) - \frac{1}{\pi} \int_0^\pi q(x) dx \right] = \frac{1}{4}[q(\pi) + q(0)] - \frac{1}{2\pi} \int_0^\pi q(x) dx. \quad (2.8)$$

Later, C.J.A. Halberg and V.A. Kramer [HK60] corrected Gel'fand and Levitan's result in the case of Robin conditions  $u'(0) = \alpha u(0)$ ,  $u'(\pi) = \beta u(\pi)$  and

they obtained the formula for the Dirichlet boundary condition and for mixed condition. We can summarize their result for the potential with a vanishing average. In the case of Neumann or Robin conditions at both ends, the formula (2.5) holds. For the Dirichlet condition at one end ( $x = 0$ ) of the interval and Neumann or Robin at the other ( $x = \pi$ ), the formula reads as

$$\sum_{n=1}^{\infty} [\lambda_n(q) - \lambda_n(0)] = \frac{1}{4}[q(\pi) - q(0)].$$

The formula for Dirichlet conditions at both ends of the interval is

$$\sum_{n=1}^{\infty} [\lambda_n(q) - \lambda_n(0)] = -\frac{1}{4}[q(\pi) + q(0)].$$

The Gelfand-Levitan trace formula for quantum graphs was studied in [Yan13, YY07], where the equilateral graphs (all the edges are of the same length) with various coupling conditions were studied, and in [Yan14], where a segment with discontinuous boundary conditions was considered.

## 2.4 Resolvent and Scattering Resonances

This section is devoted to defining resonances in quantum graphs and stating their main properties. For simplicity, we will assume the potential to be zero. The resonance is a generalization of the notion of the eigenvalue; the resonance can be a complex number. There is a small difference between resolvent and scattering resonances. Resolvent resonances are defined using the poles of the meromorphic continuation of the resolvent, while scattering resonances, the subset of resolvent resonances, are defined using the scattering matrix.

**Definition 2.1.** *The resolvent resonance  $k^2$  is a pole of the meromorphic continuation of the resolvent, the operator acting as  $(H - k^2 \text{id})^{-1}$ . Here  $k$  is the wave vector, the square root of energy, and  $\text{id}$  is the identity operator.*

The resolvent resonances can be obtained using the method of external complex scaling. The method was introduced by J. Augilar, E. Baslev, and J.-M. Combes in [AC71, BC71]. For the overview of the general theory see, e.g., [RS78]; for its application to quantum graphs see [EL07, Lip16b]. The main idea of this method is to perform the scaling transformation on the wavefunction components on the external edges  $U_\theta g_j(x) = e^{\theta/2} g_j(e^\theta x)$ , while the wavefunction components on the internal edges are not scaled. For  $\theta$  real, the above transformation is unitary. The trick, however, is to use  $\theta$  complex, with a non-trivial imaginary part, thus transforming functions that were not square integrable into square integrable ones. If we apply the transformation to the Hamiltonian, we obtain the scaled operator, which is no longer self-adjoint and its spectrum is given by the following theorem (see [Lip16b, Thms. 5.3 and 5.4]).

**Theorem 2.2.** *Let  $H_\theta = U_\theta H U_{-\theta}$  and  $f_j$ ,  $j = 1, \dots, N$  be the wavefunction components on the internal edges,  $g_j$ ,  $j = 1, \dots, M$  the wavefunction components on the external edges. Then it acts as*

$$H_\theta \begin{pmatrix} f_j(x) \\ g_j(x) \end{pmatrix} = U_\theta H U_{-\theta} \begin{pmatrix} f_j(x) \\ g_j(x) \end{pmatrix} = \begin{pmatrix} -f_j''(x) + q_j(x)f_j(x) \\ -e^{-2\theta x} g_j''(x) \end{pmatrix}.$$

*The essential spectrum of  $H_\theta$  is  $e^{-2\theta}[0, \infty)$ . The resolvent resonances of  $H$  can be obtained as eigenvalues of  $H_\theta$  for  $\text{Im } \theta$  large enough.*

The above-mentioned theorem results in an equivalent definition of resolvent resonances, which can be used for quantum graphs. For  $\text{Im } \theta > 0$  out of the two linearly independent solutions of the eigenvalue equation, only  $e^{ikx}$  is transformed into a square-integrable function. Hence the problem of finding the resolvent resonances of  $H$ , which is equivalent to finding eigenvalues of the scaled operator  $H_\theta$ , can be reformulated as the problem of finding such  $k^2$ , for which there exists a solution behaving as  $e^{ikx}$  on the external edges.

**Theorem 2.3.** *There is a resolvent resonance  $k^2$  of the operator  $H$  if and only if there exists a solution of the Schrödinger equation which satisfies the coupling conditions and has the asymptotics  $b_j e^{ikx}$  for all the external edges.*

The following theorem states that resolvent resonances can be found either in the lower complex half-plane or on the imaginary axis.

**Theorem 2.4.** *There are resonances only for  $\text{Im } k \leq 0$  or  $\text{Re } k = 0$ .*

Another way to define the resonances is to use the scattering matrix. Clearly, for a graph without potential, the solution of the Schrödinger equation on the external edges is a linear combination of the incoming wave  $e^{-ikx}$  and the outgoing wave  $e^{ikx}$ . The names “incoming” and “outgoing” are assigned to these solutions in an analogy with the corresponding solutions of the time-dependent problem (see [Lip16b]). The scattering matrix maps the vector of amplitudes of the incoming waves into the vector of amplitudes of the outgoing waves. I.e., if the solutions on the edges  $e_{j+N}$  is  $g_j(x) = a_j e^{-ikx} + b_j e^{ikx}$ , then the scattering matrix  $S$  is defined by

$$S(k)(a_1, \dots, a_M)^T = (b_1, \dots, b_M)^T.$$

The scattering resonances are defined as the poles of its determinant.

**Definition 2.5.** *The scattering resonances for a quantum graph with the scattering matrix  $S(k)$  are such  $k^2$  for which there is a pole of  $\det S(k)$ .*

The notions of resolvent and scattering resonances differ only slightly, as the following theorem ([Lip16b, Thm. 8.1]) states.

**Theorem 2.6.** *There is a resolvent resonance at  $k^2$  of  $H$  if and only if there is a scattering resonance at  $k^2$  or there is an eigenvalue at  $k^2$  with the corresponding eigenfunction supported on the internal part of the graph.*

In other words, the eigenvalue coming from the topology of the graph, which has the corresponding eigenfunction supported only on the internal edges, is a resolvent resonance, but “cannot be seen” by the scattering matrix. For more details, see [EL07, Lip16b].

## 2.5 Weyl Asymptotics

An interesting problem is to find the density of eigenvalues of a given operator. For the Dirichlet Laplacian in a bounded domain in  $\mathbb{R}^d$ , the problem was solved by H. Weyl in the series of papers from 1911 to 1915 (see, e.g. [Wey11]). He proved a formula today known as the *Weyl law* that the number of eigenvalues that are smaller than  $\lambda$  behaves as

$$N(\lambda) = \frac{1}{(2\pi)^d} \omega_d |\Omega| \lambda^{d/2} (1 + o(1)) \quad \text{as } \lambda \rightarrow \infty, \quad (2.9)$$

where  $\omega_d$  is the volume of the unit ball in  $\mathbb{R}^d$  and  $|\Omega|$  is the volume of the bounded domain. The law was previously conjectured by A. Sommerfeld [Som10] and H. Lorentz [Lor10]. Weyl also conjectured the second term of the asymptotics

$$N(\lambda) = \frac{1}{(2\pi)^d} \omega_d |\Omega| \lambda^{d/2} \mp \frac{1}{4} \frac{1}{(2\pi)^{d-1}} \omega_{d-1} |\partial\Omega| \lambda^{(d-1)/2} \quad \text{as } \lambda \rightarrow \infty,$$

where  $|\partial\Omega|$  denotes the volume of the boundary of  $\Omega$ , the upper sign corresponds to Dirichlet and the lower sign to Neumann boundary condition. The result was proven by V. Ivrii in 1980 [Ivr80]. A more detailed introduction to the history of this problem can be found in [Ivr16].

We will apply the formula (2.9) to the one-dimensional system of a quantum graph without external edges. We will work in the  $k$ -plane, i.e. study the number of eigenvalues  $N(R)$  with square roots  $k$  smaller in modulus than  $R$ . Using (2.9) one obtains

$$N(R) = \frac{2V}{\pi} R + \mathcal{O}(1), \quad (2.10)$$

where  $V$  is the sum of all edge lengths. Note that in the  $k$ -plane there are twice as many square roots of eigenvalues present than in the energy plane since there are always two square roots  $k$  for each eigenvalue.

For the graph with external edges, one can study the number of resolvent resonances present in the circle of radius  $R$  in the  $k$ -plane. Since one can construct a continuous transformation of the coupling conditions between the present case and the case when all the external edges are fully decoupled, one would expect that the eigenvalues (the resolvent resonances for the fully decoupled case) will move continuously to the complex plane and hence the formula (2.10) would hold also for the number of resonances. However, E.B. Davies and A. Pushnitski [DP11] found that this is not the case for all the graphs. In general, the formula

$$N(R) = \frac{2W}{\pi} R + \mathcal{O}(1), \quad W \leq V \quad (2.11)$$

holds. The graphs with  $W = V$  are called *Weyl*, while graphs with  $W < V$  are called *non-Weyl*, since they violate the usual Weyl formula (2.10). The reason why  $W < V$  for some of the graphs is that the resonances can, during the continuous transformation from the fully decoupled graph to the studied graph, escape to complex infinity. The value  $W$  is called the *effective size* of a graph.

A simple example of a non-Weyl graph is the graph with a vertex connecting one internal edge and one external edge with the standard condition. As follows from Section 2.2, such a vertex does not impose any interactions, since continuity of both the function values and derivatives is prescribed. Hence one can effectively replace these two edges (internal and external) with one external edge, effectively reducing the internal part of the graph. Davies and Pushnitski [DP11] found that the graph with standard coupling is non-Weyl if and only if there is a balanced vertex, the vertex connecting the same number of internal and external edges. The problem was later studied for graphs with the general coupling condition in [DEL10] and for the magnetic graphs in [EL11]. The problem of finding the effective size of a non-Weyl graph was investigated in [Lip16a] (in this thesis in Appendix E). Recently, the resonances in Weyl and non-Weyl graphs were investigated by M. Ingremeau in [Ing22a, Ing22b].

## 2.6 Pseudo-Orbit Expansion for the Graphs with External Edges

The secular equation which gives the eigenvalues of a quantum graph can be obtained by the method of pseudo-orbit expansion. The method uses the fact that the secular equation can be written using a determinant. Since the permutations in the definition of the determinant can be decomposed into particular cycles, a link to the collection of closed paths on an oriented graph can be found.

The periodic orbit expansion for quantum graphs was developed in [KS99b]. In [ACD<sup>+</sup>00], C. Akkeremans *et al* obtained a formula for the so-called spectral determinant (see Section 5.1 below) of the graph using periodic orbits noticing that some of the contributions cancel. The method of pseudo-orbit expansion for finding the secular equation for a finite quantum graph was described in [BHJ12] by R. Band, J.M. Harrison, and C.H. Joyner.

Similarly to the secular equation for finite graphs, the resonance condition for the graphs with external edges can be written. The construction of the resonance condition was done in [KS00], where also the trace formula was found. The problem was also dealt with in [GS01, Section 3]. The paper [Lip16a] presented a detailed construction of the resonance condition using the modified pseudo-orbit expansion of the paper [BHJ12]. In the rest of the section, we will briefly present the main ideas of this construction. Throughout this section, we will assume that the potential is zero.

First, we describe the effective coupling on a flower-like graph for which the external edges are cut (see e.g. [Lip16b, Thm. 9.1]).

**Theorem 2.7.** *Let the coupling on the graph  $\Gamma$  be described by a  $(2N + M) \times (2N + M)$  matrix  $U$  with the structure*

$$U = \begin{pmatrix} U_1 & U_2 \\ U_3 & U_4 \end{pmatrix},$$

where the  $2N \times 2N$  block  $U_1$  corresponds to the coupling between internal edges, the  $M \times M$  block  $U_4$  corresponds to the coupling between external edges, and the rectangular blocks  $U_2$  and  $U_3$  correspond to the mixed coupling. Let  $\lambda_i, i = 1, \dots, M$  be the eigenvalues of  $U_4$ . Then all resolvent resonances of  $\Gamma$  with the momenta  $k$  on  $\mathbb{C} \setminus \{\frac{\lambda_1-1}{\lambda_1+1}, \dots, \frac{\lambda_M-1}{\lambda_M+1}\}$  are given as eigenvalues of the operator with the same action on the internal edges but satisfying energy-dependent coupling conditions

$$(\tilde{U}(k) - I_{2N})\mathbf{f} + i(\tilde{U}(k) + I_{2N})\mathbf{f}' = 0$$

with

$$\tilde{U}(k) = U_1 - (1 - k)U_2[(1 - k)U_4 - (k + 1)I_M]^{-1}U_3, \quad (2.12)$$

where  $\mathbf{f}$  and  $\mathbf{f}'$  are the vectors of limits of function values and derivatives to the central vertex from the internal edges, respectively.

Similarly, we can define the effective coupling matrices for particular vertices of a multi-vertex graph.

Let us assume a vertex  $v$  of the graph  $\Gamma$  which connects  $n$  internal and  $m$  external edges. Let the internal edges be parametrized by  $(0, \ell_j)$  with  $x = 0$  corresponding to  $v$  and let the external edges be parametrized so that  $x = 0$  corresponds to  $v$ . Let the solutions of the Schrödinger equation be  $f_j(x) = \alpha_j^{\text{in}}e^{-ikx} + \alpha_j^{\text{out}}e^{ikx}$ ,  $j = 1, \dots, n$  on the internal edges and  $g_s(x) = \beta_s e^{ikx}$ ,  $s = 1, \dots, m$  on the external edges (we assume only the outgoing wave since we want to describe the resolvent resonances). We assume that at each vertex the coupling conditions (2.2) are satisfied.

**Definition 2.8.** *The effective vertex-scattering matrix  $\tilde{\sigma}^{(v)}$  is  $n \times n$  matrix which on the internal edges maps the vectors of incoming waves into the vector of outgoing waves  $\vec{\alpha}_v^{\text{out}} = \tilde{\sigma}^{(v)}\vec{\alpha}_v^{\text{in}}$ , where  $\vec{\alpha}_v^{\text{in}}$  and  $\vec{\alpha}_v^{\text{out}}$  are vectors with entries  $\alpha_j^{\text{in}}$  and  $\alpha_j^{\text{out}}$ , respectively.*

We state a theorem ([Lip16a, Thm. 4.2] and [Lip16b, Lemma 12.2]) about the relation between the effective coupling matrix and the effective vertex-scattering matrix. For simplicity, we drop the sub- (super-) script  $v$ .

**Theorem 2.9.** *Let us consider a graph  $\Gamma$  with the vertex  $v$ , the unitary matrix  $U$  describing the coupling (2.2) in  $v$  and the effective vertex-scattering matrix  $\tilde{\sigma}(k)$  at  $v$ . Let  $\tilde{U}(k)$  be the effective coupling matrix at  $v$  defined by (2.12). Then the effective vertex-scattering matrix is given by*

$$\tilde{\sigma}(k) = -[(1 - k)\tilde{U}(k) - (1 + k)I_n]^{-1}[(1 + k)\tilde{U}(k) - (1 - k)I_n].$$

The inverse relation is

$$\tilde{U}(k) = [(1 + k)\tilde{\sigma}(k) + (1 - k)I_n][(1 - k)\tilde{\sigma}(k) + (1 + k)I_n]^{-1}.$$

For the purposes of the pseudo-orbit expansion, we define an oriented graph  $\Gamma_2$ . It can be obtained from the graph  $\Gamma$  when each finite edge  $e_j$  is replaced by two oriented edges (which we will call *bonds*)  $b_j$  and  $\hat{b}_j$  which have the opposite orientation and both of them have the same length as  $e_j$ . If the edge  $e_j$  is parametrized so that  $x = 0$  corresponds to the vertex  $v_{j1}$  and  $x = \ell_j$  to the vertex  $v_{j2}$ , we parametrize the bonds so that  $b_j$  starts at  $v_{j1}$  and ends at  $v_{j2}$  and  $\hat{b}_j$  starts at  $v_{j2}$  and ends at  $v_{j1}$ .

Now we construct the resonance condition similarly to [BHJ12, Lip16a, Lip16b, Lip15]. We define matrices  $\tilde{\Sigma}(k)$  and  $\tilde{S}(k)$  similarly to [Lip16b].

**Definition 2.10.** *The matrix  $\tilde{\Sigma}(k)$  is an energy-dependent block-diagonalizable  $2N \times 2N$  matrix with blocks  $\tilde{\sigma}^v(k)$ . The similarity transformation, under which the matrix is block-diagonal, is given as a transformation between the basis*

$$\vec{\alpha} = (\alpha_{b_1}^{\text{in}}, \dots, \alpha_{b_N}^{\text{in}}, \alpha_{\hat{b}_1}^{\text{in}}, \dots, \alpha_{\hat{b}_N}^{\text{in}})^{\text{T}}$$

and the basis

$$(\alpha_{b_{v_1 1}}^{\text{in}}, \dots, \alpha_{b_{v_1 d_1}}^{\text{in}}, \alpha_{b_{v_2 1}}^{\text{in}}, \dots, \alpha_{b_{v_2 d_2}}^{\text{in}}, \dots)^{\text{T}},$$

where  $b_{v_1 j}$  is the  $j$ -th edge ending in the vertex  $v_1$ .

The scattering matrix is  $\tilde{S}(k) = Q\tilde{\Sigma}(k)$ , where  $Q = \begin{pmatrix} 0 & I_N \\ I_N & 0 \end{pmatrix}$ . The matrix  $I_N$  denotes the identity  $N \times N$  matrix. Moreover, we define

$$L = \text{diag}(\ell_1, \dots, \ell_N, \ell_1, \dots, \ell_N).$$

Further, we use on the oriented graph the ansatz

$$\begin{aligned} f_{b_j}(x) &= \alpha_{b_j}^{\text{in}} e^{-ikx_{b_j}} + \alpha_{b_j}^{\text{out}} e^{ikx_{b_j}}, \\ f_{\hat{b}_j}(x) &= \alpha_{\hat{b}_j}^{\text{in}} e^{-ikx_{\hat{b}_j}} + \alpha_{\hat{b}_j}^{\text{out}} e^{ikx_{\hat{b}_j}}, \end{aligned}$$

where  $x_{b_j}$  and  $x_{\hat{b}_j}$  are the coordinates on the bonds  $b_j$  and  $\hat{b}_j$ , respectively. Since the oriented graph corresponds to the non-oriented graph  $\Gamma$ , we have  $x_{b_j} + x_{\hat{b}_j} = \ell_j$  with  $\ell_{b_j} \equiv \ell_j$ . Moreover, the function values on the corresponding bonds must correspond to each other,  $f_{b_j}(x_{b_j}) = f_{\hat{b}_j}(\ell_j - x_{\hat{b}_j})$ . Hence for the coefficients in the above ansatz we obtain

$$\alpha_{b_j}^{\text{in}} = e^{ik\ell_j} \alpha_{\hat{b}_j}^{\text{out}}, \quad \alpha_{\hat{b}_j}^{\text{in}} = e^{ik\ell_j} \alpha_{b_j}^{\text{out}}. \quad (2.13)$$

We define  $\vec{\alpha}_b^{\text{in}} = (\alpha_{b_1}^{\text{in}}, \dots, \alpha_{b_N}^{\text{in}})^{\text{T}}$  and similarly for the outgoing amplitudes and bonds in the opposite direction  $\hat{b}_j$ . Using the relations (2.13) and the definitions of matrices  $Q$  and  $\tilde{\Sigma}$  we obtain the following

$$\begin{pmatrix} \vec{\alpha}_b^{\text{in}} \\ \vec{\alpha}_{\hat{b}}^{\text{in}} \end{pmatrix} = e^{ikL} \begin{pmatrix} \vec{\alpha}_b^{\text{out}} \\ \vec{\alpha}_{\hat{b}}^{\text{out}} \end{pmatrix} = e^{ikL} Q \begin{pmatrix} \vec{\alpha}_b^{\text{out}} \\ \vec{\alpha}_{\hat{b}}^{\text{out}} \end{pmatrix} = e^{ikL} Q \tilde{\Sigma}(k) \begin{pmatrix} \vec{\alpha}_b^{\text{in}} \\ \vec{\alpha}_{\hat{b}}^{\text{in}} \end{pmatrix}.$$

This yields the following theorem ([Lip16a, Thm. 4.5], [Lip16b, Thm. 13.5]).



**Theorem 2.11.** *The resonance condition is given by*

$$\det(e^{ikL}Q\tilde{\Sigma}(k) - I_{2N}) = 0.$$

The construction in [Lip16a] at this stage follows the machinery developed in [BHJ12] and rewrites the determinant using the pseudo-orbits defined below. We copy the definition from [Lip16b].

**Definition 2.12.** *Let us describe the bond  $b$  by end vertices  $b = (u, v)$ ; let the origin be  $o(b) = u$  and terminus  $t(b) = v$ . A periodic orbit  $\gamma$  on the graph  $\Gamma_2$  is a closed path that begins and ends in the same vertex. We can denote it by the bonds that it subsequently contains, e.g.  $\gamma = (b_1, b_2, \dots, b_n)$ ; this means  $t(b_i) = o(b_{i+1})$ ,  $i = 1, \dots, n-1$  and  $t(b_n) = o(b_1)$ . The cyclic permutation of bonds does not change the periodic orbit. A pseudo-orbit is a collection of periodic orbits ( $\tilde{\gamma} = \{\gamma_1, \gamma_2, \dots, \gamma_m\}$ ). An irreducible pseudo-orbit  $\bar{\gamma}$  is a pseudo-orbit that does not contain any bond more than once. The metric length of a periodic orbit is defined as  $\ell_\gamma = \sum_{b_j \in \gamma} \ell_{b_j}$ ; the length of a pseudo-orbit is the sum of the lengths of all periodic orbits the pseudo-orbit is composed of. We denote the product of scattering amplitudes along the periodic orbit  $\gamma = (b_1, b_2, \dots, b_n)$  as  $A_\gamma = S_{b_2 b_1} S_{b_3 b_2} \dots S_{b_1 b_n}$ , where  $S_{b_i b_j}$  denotes the entry of the matrix  $S(k)$  in the row corresponding to the bond  $b_i$  and column corresponding to the bond  $b_j$ . For a pseudo-orbit we define  $A_{\bar{\gamma}} = \prod_{\gamma_j \in \bar{\gamma}} A_{\gamma_j}$ . By  $m_{\bar{\gamma}}$  we denote the number of periodic orbits in the pseudo-orbit  $\bar{\gamma}$ . The set of irreducible pseudo-orbits also contains the null orbit, an irreducible pseudo-orbit on zero edges, with  $m_{\bar{\gamma}} = 0$ ,  $\ell_{\bar{\gamma}} = 0$  and  $A_{\bar{\gamma}} = 1$ .*

With these definitions at hand, we can rewrite Theorem 2.11 as below, see [Lip16b, Thm. 12.6], [Lip16a, 4.7].

**Theorem 2.13.** *The condition for the resolvent resonances of the graph is given by*

$$\sum_{\bar{\gamma}} (-1)^{m_{\bar{\gamma}}} A_{\bar{\gamma}}(k) e^{ik\ell_{\bar{\gamma}}} = 0,$$

where the sum goes over all irreducible pseudo-orbits  $\bar{\gamma}$ .

## 2.7 Fermi Golden Rule

Fermi golden rule is in physics usually understood as a formula giving the transition rate from the initial to the final state. However, an alternative approach is possible. It can be connected with the second derivative of the imaginary part of the resonance position with respect to a given parameter (see, e.g. [RS78, Theorem XII.24], [Lip16b, Sec. 18]). This approach was studied in the paper [LZ16], where a formula was found for the second derivative of the imaginary part of the resonance with respect to the parameter  $t$  connected with the lengths of the graph's edges. Their study uses graphs with standard coupling conditions and

without potential and the mentioned notion is obtained in the terms of eigenfunction  $u$  corresponding to one of the eigenvalues  $\lambda$  for  $t = 0$  and the generalized eigenfunctions.

We emphasize that by indices  $j = 1, \dots, N$  we denote the internal edges and by indices  $j = N + 1, \dots, N + M$  the external ones.

**Definition 2.14.** *The generalized eigenfunctions  $e^s(k)$ ,  $N + 1 \leq s \leq N + M$  are for  $k^2 \notin \sigma_{\text{pp}}(H)$  defined as*

$$\begin{aligned} e^s(k) &\in \mathcal{D}_{\text{loc}}(H), \quad (H - k^2)e^s(k) = 0, \\ e_j^s(k, x) &= \delta_{js}e^{-ikx} + s_{js}(k)e^{ikx}, \quad N + 1 \leq j \leq N + M, \end{aligned}$$

where  $e_j^s$  are the components of  $e^s$  on the external edges and  $\mathcal{D}_{\text{loc}}(H)$  is the space of functions that are locally in the domain of  $H$ . This family of generalized eigenfunctions can be holomorphically extended to the points of the spectrum of  $H$  and therefore it is defined for all  $k$ .

The edge lengths of the graph depend on the parameter  $t$  as

$$\ell_j(t) = e^{-a_j(t)}\ell_j, \quad a_j(0) = 0,$$

where  $a_j$  are real functions of  $t$ .

Then the result of [LZ16, Thm. 1] is the following (we copy the formulation from [Lip16b]).

**Theorem 2.15.** *Consider a simple eigenvalue  $k_0^2 > 0$  of the Hamiltonian  $H \equiv H(0)$  and let  $u$  be the corresponding eigenfunction. Then for  $|k| \leq k_{\text{max}}$  there exists a smooth function  $t \mapsto k(t)$  such that  $k^2(t)$  is the resolvent resonance of  $H(t)$ . Moreover, we have*

$$\begin{aligned} \text{Im } \ddot{k}(0) &= - \sum_{s=N+1}^{N+M} |F_s|^2, \\ F_s &= k_0 \langle \dot{a}u, e^s(k_0) \rangle + \frac{1}{k_0} \sum_{v \in \Gamma} \sum_{e_j \ni v} \frac{1}{4} \dot{a}_j (3\partial_\nu u_j(v) \overline{e_j^s(k, v)} - u(v) \partial_\nu \overline{e_j^s(k, v)}), \end{aligned}$$

where the double dot denotes the second derivative with respect to  $t$ ,  $\dot{a}$  is the first derivative of the function  $a$  with components  $a_j(t)$ ,  $\langle \bullet, \bullet \rangle$  is the inner product in  $\oplus_{j=1}^N L^2([0, \ell_j]) \oplus \oplus_{s=N+1}^{N+M} L^2([0, \infty))$ , the sum  $\sum_{v \in \Gamma}$  goes through all the vertices of the graph  $\Gamma$ ,  $\partial_\nu u_j(0) = -u_j'(0)$  and  $\partial_\nu u_j(\ell_j) = u_j'(\ell_j)$ .

## 2.8 Results on Quantum Graphs

In this section, we introduce the main results of papers in appendices A–E.

### 2.8.1 Spectral Asymptotics of the Laplacian on Platonic Solids Graphs

The first paper [EL19] (see Appendix A) illustrates the different properties of the preferred-orientation coupling for finite graphs having the vertices and edges of Platonic solids. Five equilateral graphs having the edges and vertices of the tetrahedron, cube, octahedron, dodecahedron, and icosahedron were considered. The paper can be motivated by the shapes of various molecules, such as methane for the tetrahedron, cubane for the cube, SF<sub>6</sub> for the octahedron, dodecahedrane for the dodecahedron, or boron for the icosahedron.

Two types of coupling conditions are considered at the vertices of the Platonic solid graphs – the  $\delta$ -coupling with the same coupling constant at all the vertices and the preferred-orientation coupling with the same orientation of the vertices if seen from the outside. The asymptotic positions of the eigenvalues of the Laplacian on the graphs were investigated. For the  $\delta$ -coupling, the square roots of eigenvalues approach those for the standard coupling condition. The square root of the  $n$ -th eigenvalue for the  $\delta$ -condition differs from the square root of the  $n$ -th eigenvalue for standard coupling by the term of order  $\mathcal{O}(1/n)$ . Since the differential of the energy is  $dE = 2k dk$  and  $k$  scales as  $n$ , the  $\mathcal{O}(1/n)$  difference between the square roots means that the distance of the eigenvalues for  $\delta$  and standard coupling is at most asymptotically constant.

For the preferred-orientation coupling, the dependence of the spectral properties on parity was observed. The only Platonic solid graph with an even degree of the vertices is the octahedron graph (degree 4), while all the other four Platonic solid graphs have vertices of odd degree (tetrahedron, cube, and dodecahedron have vertices of degree 3; the icosahedron has degree 5). We found that, as was expected, the square roots of eigenvalues for odd-degree graphs converge to those of the Neumann Laplacian on the interval of length one. This follows from the fact that the vertex scattering matrices approach for large energies the identity matrix and the graph is thus effectively decoupled to single edges. As in the case of  $\delta$ -condition, the error term for the square roots is of order  $\mathcal{O}(1/n)$ , hence the distance of the eigenvalues for the preferred-orientation coupling from the eigenvalues of the interval with Neumann conditions is at most a given constant. As an example of an odd-degree graph, we give the corresponding theorem for the tetrahedron.

**Theorem 2.16.** *For the tetrahedron with the preferred-orientation coupling, the (square roots of) eigenvalues  $k$  are for large  $k$  contained in the intervals*

$$k_n \in \left( n\pi - \frac{2\sqrt{3}}{n\pi} + \mathcal{O}\left(\frac{1}{n^2}\right), n\pi + \frac{2\sqrt{3}}{n\pi} + \mathcal{O}\left(\frac{1}{n^2}\right) \right), \quad n \in \mathbb{Z}.$$

The octahedron has different behaviour. Since the degree of its vertices is even, there is approximately the same probability of reflection and transmission through the vertices for large energies. The square roots of eigenvalues can asymptotically

appear at different positions than for the other Platonic solid graphs, as the following theorem states.

**Theorem 2.17.** *The (square roots of) eigenvalues for the octahedron with the preferred-orientation coupling are at  $k = 2\pi n$  (with multiplicity eight) and  $k = \pm\frac{2}{3}\pi + 2\pi n$  (with multiplicity two) with  $n \in \mathbb{Z}$ ; the other (square roots of) eigenvalues are situated in the intervals*

$$k_n^{(1)} \in \left[ \pi + 2\pi n - \frac{\sqrt{10}}{\pi + 2\pi n} + \mathcal{O}\left(\frac{1}{n^2}\right), \pi + 2\pi n + \frac{\sqrt{10}}{\pi + 2\pi n} + \mathcal{O}\left(\frac{1}{n^2}\right) \right],$$

$$k_n^{(2)} \in \left[ \frac{\pi}{2} + \pi n - \frac{5}{\left(\frac{\pi}{2} + \pi n\right)^2} + \mathcal{O}\left(\frac{1}{n^4}\right), \frac{\pi}{2} + \pi n + \frac{5}{\left(\frac{\pi}{2} + \pi n\right)^2} + \mathcal{O}\left(\frac{1}{n^4}\right) \right].$$

## 2.8.2 Topological Bulk-Edge Effects in Quantum Graph Transport

The second publication [EL20] (see Appendix B) also deals with quantum graphs with preferred-orientation coupling. However, in this paper, the graphs have infinitely many internal edges. Two types of lattices are defined and from each of them, a straight strip is cut. The lattices are designed such that the parity of the vertices differs for vertices at the edge of the strip and in the bulk, i.e. in the middle of the strip. This results in different high-energy behaviour of the spectra of these graphs and hence different transport properties of the strips.

The rectangular lattice (see Fig. 2.3a) has vertices of degree 3 at the edge of the strip and vertices of degree 4 in the middle. Let the lengths of its vertical edges be  $\ell_2$ . For the momentum  $k$  (square root of the energy) not close to multiples of  $\pi/\ell_2$  the transport near the edge is not possible. The generalized eigenfunction components at the leftmost and rightmost edge are of order  $\mathcal{O}(1/k)$ , as the following theorem states. Its proof uses the fact that the vertex-scattering matrix for the vertices of the edge of the strip is the identity matrix.

**Theorem 2.18.** *Let us consider the rectangular lattice. For a fixed  $K \in (0, \frac{1}{2}\pi)$ , consider momenta  $k > 0$  such that  $k \notin \bigcup_{n \in \mathbb{N}_0} \left( \frac{n\pi - K}{\ell_2}, \frac{n\pi + K}{\ell_2} \right)$ . Suppose that the restriction of the generalized eigenfunction corresponding to energy  $k^2$  to the elementary cell is normalized, then its components at the leftmost and rightmost vertical edges are at most of order  $\mathcal{O}(k^{-1})$ .*

On the other hand, the situation for the “brick” lattice (see Fig. 2.3b) is the opposite. The lattice is constructed so that the only vertices having an even degree (in particular 4) are the vertices of the leftmost vertical edges. The other vertices have degree 3 or 5, including the vertices of the rightmost edges. Let us denote by  $q_j^{(m)}$  the coefficients of the components of the generalized eigenfunctions in the  $j$ -th cell. The index  $j$  denotes the distance of the cell from the left, i.e. the left-most cell has  $j = 1$ , the neighbouring has  $j = 2$ , etc. The index  $m$  denotes

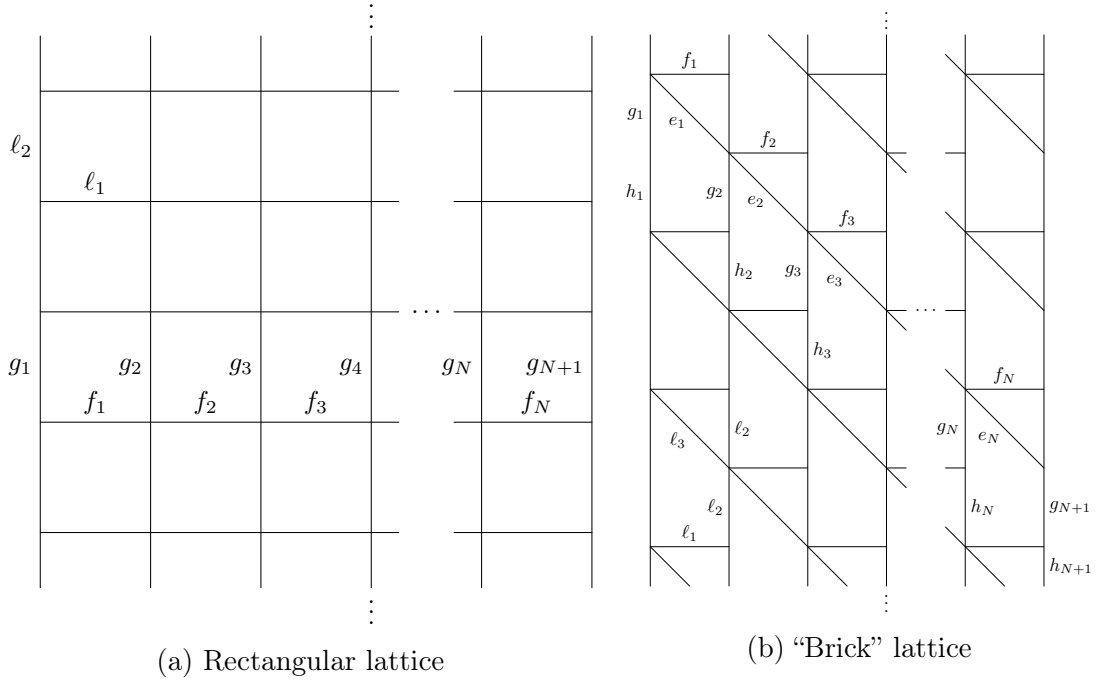


Figure 2.3: Rectangular (left) and "brick" (right) lattice strips. Reproduced from [EL20].

the edge in the cell. The following theorem states that the coefficients  $q_j^{(m)}$  for momenta  $k$  far from multiples  $\pi/\ell_i$ , where  $\ell_i, i = 1, 2, 3$  are the edge lengths, are of order  $\mathcal{O}(k^{1-j})$ . The generalized eigenfunction exponentially decays with the distance from the leftmost edge.

**Theorem 2.19.** *Let us consider the "brick" lattice. For a fixed  $K \in (0, \frac{1}{2}\pi)$ , consider momenta  $k > 0$  such that*

$$k \notin \bigcup_{n \in \mathbb{N}_0} \left( \frac{n\pi - K}{\ell_1}, \frac{n\pi + K}{\ell_1} \right) \cup \bigcup_{n \in \mathbb{N}_0} \left( \frac{n\pi - K}{\ell_2}, \frac{n\pi + K}{\ell_2} \right) \cup \bigcup_{n \in \mathbb{N}_0} \left( \frac{n\pi - K}{\ell_3}, \frac{n\pi + K}{\ell_3} \right). \quad (2.14)$$

*Suppose again that the restriction of the generalized eigenfunction corresponding to energy  $k^2$  to the elementary cell is normalized, then  $q_j^{(m)}$  is at most of order  $\mathcal{O}(k^{1-j})$  as  $k \rightarrow \infty$ .*

The main idea of the proofs of both theorems is Floquet-Bloch decomposition. Then the ansatzes on the edges were sewed by the coupling conditions and the fact that the scattering matrix for an odd-degree vertex is an identity matrix was used. The theoretical results were supported numerically. First, we obtained the dispersion diagrams for both lattices for  $k$  slightly larger than 100. Then for three cells in the rectangular lattice case and for two cells in the "brick" lattice case, we obtained the graphs of probability current through the edges and of the sum of squares of wavefunction components coefficients. Both notions differ between

neighbouring cells by several orders of magnitude. We obtained the “edge states” for the “brick” lattice (the states supported mainly near the edge of the strip); however, the system is not an example of a topological insulator, because the probability current can move in both directions for various values of the Floquet parameter.

### 2.8.3 A Gelfand-Levitan Trace Formula for Generic Quantum Graphs

In the paper [FL21] in Appendix C, a generalization of the Gelfand-Levitan trace formula for graphs was made. The graphs considered in this paper are generic in the following sense: all coupling matrices  $U$  (see equation (2.3)) which do not have the eigenvalue  $-1$  are considered. The excluded set of the Dirichlet part of the coupling is a set of measure zero in the family of all coupling conditions; however, it includes some important cases, such as, for instance, Dirichlet, standard or  $\delta$ -condition. We should stress that in view of the results of C.J.A. Halberg and V.A. Kramer [HK60] (see Section 2.3) for the excluded set of coupling conditions the formula presented below does not hold.

The paper generalizes previous results by C.-F. Yang and J.-X. Yang [YY07, Yan13, Yan14] in several directions. Firstly, the set of considered coupling conditions is significantly larger; the generic case is studied in [FL21] in contrast to particular coupling conditions in the works of Yang and Yang. Our generic case also includes various topologies of the graph (see the remark on the “flower-like” graph in Section 2.1). Moreover, there are general edge lengths considered in [FL21], the only restriction is that the edge lengths are positive. We should also mention that our result is closer to the formulation of the original Gelfand-Levitan formula; in the sum, we subtract the eigenvalue of the operator without the potential. The results of Yang and Yang are different, they subtract a particular  $n$ -dependent expression.

Before formulating the main result of this paper, we define the sequences of eigenvalues that will be used in the Gelfand-Levitan formula. Let us consider a quantum graph with  $N$  internal edges of lengths  $\ell_i$ ,  $i = 1, \dots, N$  and no external edge. Let there be the potential  $q$  with edge components  $q_i \in W^{1,1}((0, \ell_i))$  on the graph. Under the assumption that the coupling matrix  $U$  does not have an eigenvalue  $-1$ , one can find that the leading term of the secular equation (the equation giving the eigenvalues of the problem) is  $\prod_{i=1}^N (-k \sin k\ell_i)$ . We define  $N$  sequences of eigenvalues  $\lambda_{in}$  in the following way. Let the sequence of all eigenvalues of the problem in increasing order be  $\{\lambda_n(q)\}_{n=1}^\infty \equiv \{\lambda_n\}_{n=1}^\infty$  and let the sequence  $\{\mu_n\}_{n=1}^\infty$  correspond to non-negative zeros of the product  $\prod_{i=1}^N (-k \sin k\ell_i)$  in increasing order, where the first  $N$  entries  $\mu_1, \dots, \mu_N$  are zeros. We pair the corresponding entries of both sequences. Then we define the sequences  $\{\lambda_{in}\}_{n=1}^\infty$  as the subsequences of  $\{\lambda_n\}_{n=1}^\infty$  which are paired with such entries of the sequence  $\{\mu_n\}_{n=1}^\infty$  that are non-negative zeros of  $\sin k\ell_i$  for a given  $i$ . The first entry is paired with a zero.

**Theorem 2.20.** *We assume a quantum graph with  $N$  edges with arbitrary lengths  $\ell_i$ ,  $i = 1, \dots, N$ , and associated coupling matrix  $U$  not having  $-1$  in its spectrum. Then, denoting the eigenvalues of the Hamiltonian with a potential  $q$  and with the zero potential by  $\lambda_{in}(q)$  and  $\lambda_{in}(0)$ , respectively, in the way described above, and the component of the potential on the  $i$ -th edge by  $q_i \in W^{1,1}((0, \ell_i))$ , the following trace formula holds*

$$\sum_{i=1}^N \sum_{n=0}^{\infty} \left[ \lambda_{in}(q) - \lambda_{in}(0) - \frac{1}{\ell_i} \int_0^{\ell_i} q_i(x) dx \right] = \sum_{i=1}^N \left\{ \frac{1}{4} [q_i(\ell_i) + q_i(0)] - \frac{1}{2\ell_i} \int_0^{\ell_i} q_i(x) dx \right\}.$$

The result is closely related to the original Gelfand-Levitan trace formula formulated for the potential with non-zero average (2.8). The assumption  $-1 \notin \sigma(U)$  is essential, otherwise the formula is different.

#### 2.8.4 Pseudo-Orbit Approach to Trajectories of Resonances in Quantum Graphs with General Vertex Coupling: Fermi Rule and High-Energy Asymptotics

The paper [EL17] in Appendix D uses the pseudo-orbit expansion to obtain the results on the positions and trajectories of resolvent resonances in quantum graphs. First, a formula for the Fermi golden rule for graphs with general coupling conditions is obtained. The formula is a bit technical and is not as elegant as the one in [LZ16]. On the other hand, it can be applied to the general coupling conditions.

Below, we give one of the paper's main theorems. Its corollary gives the values of the real and imaginary parts of the first and second derivatives with respect to the parameter  $t$ . We will not present it here and we refer the reader to Appendix D.

**Theorem 2.21.** *Let the internal edge lengths of the graph  $\ell_j = \ell_j(t)$  depend on the parameter  $t$  as  $C^2$  functions. Suppose that at least some of them are non-constant in the vicinity of  $t = 0$  and that at that point the system has an eigenvalue  $k_0^2 > 0$  embedded in the continuous spectrum. Then for small enough  $t$  the resonance condition has the unique solution  $k^2$ , either an embedded eigenvalue or a resonance, and the following holds:*

- (i)  $\dot{k} \in \mathbb{R}$ , where the dot signifies the derivative with respect to  $t$ .
- (ii) Furthermore, we have

$$\dot{k} \sum_{\bar{\gamma}} \left( \ell_{\bar{\gamma}} A_{\bar{\gamma}}(k) - i \frac{\partial A_{\bar{\gamma}}(k)}{\partial k} \right) (-1)^{m_{\bar{\gamma}}} e^{ik\ell_{\bar{\gamma}}} + k \sum_{\bar{\gamma}} \dot{\ell}_{\bar{\gamma}} (-1)^{m_{\bar{\gamma}}} A_{\bar{\gamma}}(k) e^{ik\ell_{\bar{\gamma}}} = 0,$$

and

$$\begin{aligned}
 & \ddot{k} \sum_{\bar{\gamma}} \left( \ell_{\bar{\gamma}} A_{\bar{\gamma}}(k) - i \frac{\partial A_{\bar{\gamma}}(k)}{\partial k} \right) (-1)^{m_{\bar{\gamma}}} e^{ik\ell_{\bar{\gamma}}} \\
 & + 2\dot{k} \sum_{\bar{\gamma}} \left( ik\ell_{\bar{\gamma}} \dot{\ell}_{\bar{\gamma}} A_{\bar{\gamma}}(k) + \dot{\ell}_{\bar{\gamma}} A_{\bar{\gamma}}(k) + k\dot{\ell}_{\bar{\gamma}} \frac{\partial A_{\bar{\gamma}}(k)}{\partial k} \right) (-1)^{m_{\bar{\gamma}}} e^{ik\ell_{\bar{\gamma}}} \\
 & + (\dot{k})^2 \sum_{\bar{\gamma}} \left( 2\ell_{\bar{\gamma}} \frac{\partial A_{\bar{\gamma}}(k)}{\partial k} - i \frac{\partial^2 A_{\bar{\gamma}}(k)}{\partial k^2} + i\ell_{\bar{\gamma}}^2 A_{\bar{\gamma}}(k) \right) (-1)^{m_{\bar{\gamma}}} e^{ik\ell_{\bar{\gamma}}} \\
 & + k \sum_{\bar{\gamma}} (\ddot{\ell}_{\bar{\gamma}} + ik(\dot{\ell}_{\bar{\gamma}})^2) A_{\bar{\gamma}}(k) (-1)^{m_{\bar{\gamma}}} e^{ik\ell_{\bar{\gamma}}} = 0,
 \end{aligned}$$

where the sum goes through the irreducible pseudo-orbits.

The second set of the main results is connected with the asymptotic positions of the resonances for large energies. First, we give the theorem on the  $\delta$ -condition.

**Theorem 2.22.** *Consider a graph  $\Gamma$  with the  $\delta$ -coupling at all the vertices. Its resonances converge to the resonances of the same graph with the standard conditions as their real parts tend to infinity.*

The next two theorems deal with the  $\delta'_s$ -condition at the vertices, where external edges are attached.

**Theorem 2.23.** *The resonances of the graph with the  $\delta'_s$ -coupling conditions at the vertices converge to the eigenvalues of the graph with Neumann (decoupled) conditions as their real parts tend to infinity.*

**Theorem 2.24.** *The resonances of the graph with  $\delta'_s$  coupling conditions at the vertices, where the external edges are attached, and arbitrary self-adjoint coupling at the other vertices satisfy*

$$\operatorname{Im} k \rightarrow 0 \quad \text{as} \quad |k| \rightarrow \infty.$$

Examples for both types of results are given in the paper: the trajectories of resonances near the eigenvalue for particular quantum graphs and positions of resonances for large momenta.

### 2.8.5 On the Effective Size of a Non-Weyl Graph

The paper in Appendix E deals with the resolvent resonances for a graph with external edges and gives results for the effective size of a graph with non-Weyl asymptotics (see Section 2.5). First, the pseudo-orbit expansion for non-compact quantum graphs was developed in this paper. It is the first use of the pseudo-orbit method for quantum graphs with external edges, though the resonance condition from Thm. 2.11 was obtained e.g. in [KS00, GS01]. The theory was introduced in Section 2.6.



Moreover, the effective size of a non-Weyl graph was studied and the following results [Lip16a, Thms. 5.2, 5.3 and Cor. 5.4] on its value were obtained (for the notation, see Section 2.6).

**Theorem 2.25.** *A graph is non-Weyl iff  $\det \tilde{\Sigma}(k) = 0$  for all  $k \in \mathbb{C}$ . In other words, a graph is non-Weyl iff there exists a vertex for which  $\det \tilde{\sigma}_v(k) = 0$  for all  $k \in \mathbb{C}$ .*

For an equilateral graph (a graph that has all the internal edges of the same length) we obtained the following theorem and corollary.

**Theorem 2.26.** *Let us assume an equilateral graph (all internal edges have lengths  $\ell$ ). Then the effective size of this graph is  $\frac{\ell}{2}n_{\text{nonzero}}$ , where  $n_{\text{nonzero}}$  is the number of nonzero eigenvalues of the matrix  $Q\tilde{\Sigma}(k)$ .*

**Corollary 2.27.** *Let  $\Gamma$  be an equilateral graph with standard coupling and with  $n_{\text{bal}}$  balanced vertices. Then the effective size  $W < \text{vol } \Gamma - \frac{\ell}{2}n_{\text{bal}}$  iff  $\text{rank}(Q\tilde{\Sigma}Q\tilde{\Sigma}) < \text{rank}(Q\tilde{\Sigma}) = 2N - n_{\text{bal}}$ .*

In the next part of the paper, we developed a method of deleting some edges of the oriented graph for a non-Weyl graph  $\Gamma$  and thus simplifying the pseudo-orbit expansion for this graph. As the main results, we obtained bounds on the effective size of an equilateral graph [Lip16a, Thms. 7.1 and 7.2] below and stated a theorem on the positions of the resonances.

**Theorem 2.28.** *Let us assume an equilateral graph with  $N$  internal edges of lengths  $\ell$ , with standard coupling,  $n_{\text{bal}}$  balanced vertices, and  $n_{\text{nonneig}}$  balanced vertices that do not neighbor any other balanced vertex. Then the effective size is bounded by  $W \leq N\ell - \frac{\ell}{2}n_{\text{bal}} - \frac{\ell}{2}n_{\text{nonneig}}$ .*

**Theorem 2.29.** *Let us assume an equilateral graph ( $N$  internal edges of the lengths  $\ell$ ) with standard coupling. Let there be a square of balanced vertices  $v_1, v_2, v_3$  and  $v_4$  without diagonals, i.e.  $v_1$  neighbors  $v_2, v_2$  neighbors  $v_3, v_3$  neighbors  $v_4, v_4$  neighbors  $v_1, v_1$  does not neighbor  $v_3$  and  $v_2$  does not neighbor  $v_4$ . Then the effective size is bounded by  $W \leq (N - 3)\ell$ .*

Furthermore, examples explaining the procedures are given in the paper.

# Chapter 3

## Microwave Graphs

Although quantum graphs are a good model for describing the behaviour of a quantum particle, performing quantum experiments can be difficult and expensive. A good opportunity to model a quantum graph is to study microwaves in coaxial cables. Since the Schrödinger equation without potential is up to constants equivalent to the telegraph equation valid for the propagation of microwaves, the so-called microwave graphs can serve as a good test for quantum graph theory.

The microwave graphs are studied mainly by the group of L. Sirko from the Polish Academy of Sciences, which has published dozens of papers on the topic, starting from the seminal paper [HBP<sup>+</sup>04]; from the other papers we mention e.g. [HLB<sup>+</sup>12, LSB<sup>+</sup>14, LLS19, LKB<sup>+</sup>21]. Another group that investigates microwave graphs is the group of H.-J. Stöckmann from Philipps-Universität Marburg [AGB<sup>+</sup>14, RAJ<sup>+</sup>16].

### 3.1 Description of the Model and Setup

We briefly describe the microwave graphs that are used by the group of L. Sirko. The microwave networks are built from coaxial cables and T-junctions. The cables consist of two conductors, the inner conductor has the radius 0.05 cm, the outer conductor has the inner radius 0.15 cm. Between the conductors, there is teflon with the dielectric constant  $\varepsilon \approx 2.06$ . The lengths of the quantum graphs which correspond to the microwave network are given by the so-called optical length  $\ell_j = \ell_j^g \sqrt{\varepsilon}$ , where  $\ell_j^g$  is the geometric length of the cables.

The potential difference between the conductors  $U_{ij}(x, t)$  has the form  $U_{ij}(x, t) = e^{-i\omega t} U_{ij}(x)$ , where  $\omega$  is the angular frequency. In an ideal lossless cable with zero resistance its space component  $U_{ij}(x)$  satisfies the equation

$$\frac{d^2}{dx^2} U_{ij}(x) + \frac{\omega^2 \varepsilon}{c^2} U_{ij}(x) = 0, \quad (3.1)$$

where  $c$  is the velocity of light. For more details, see e.g. [HBP<sup>+</sup>04]. This telegraph equation is equivalent to the time-independent Schrödinger equation

with zero potential (taken in the set of units  $\hbar = 2m = 1$ )

$$\frac{d^2}{dx^2}\psi_{ij}(x) + k^2\psi_{ij}(x) = 0. \quad (3.2)$$

In both equations the indices  $i, j$  in  $U_{ij}(x)$  and  $\psi_{ij}(x)$  correspond to the edge connecting  $i$ -th and  $j$ -th vertex of the graph. The equivalence of equations (3.1) and (3.2) can be obtained under the correspondence  $U_{ij}(x) \leftrightarrow \psi_{ij}(x)$  and  $\frac{\omega\sqrt{\epsilon}}{c} \leftrightarrow k$ .

In the experiment, one can, of course, perform the measurement only with real momenta. Since the scattering matrix for quantum graphs is unitary, the absolute value of its determinant is equal to one for all  $k$ . Hence the resonances cannot be seen by the scattering matrix in the ideal lossless case. Luckily, there are always losses present and the resonances appear as peaks (to be more precise, abrupt lowering of the absolute value of the scattering matrix determinant). The closer the resonance to the real axis, the thinner the peak. In an experiment, we aim to avoid two resonances with approximately the same real parts. These resonances can be hardly distinguished from each other by the scattering data.

## 3.2 Results on Microwave Graphs

This section will be devoted to two results on microwave graphs presented in Appendices F and G.

### 3.2.1 Non-Weyl Microwave Graphs

In the paper [LLS19] in Appendix F, the problem of non-Weyl resonance asymptotics is studied numerically and experimentally. Two graphs with the same internal part were investigated. The graphs differ in the position of the vertices, where the external edges were attached. The standard coupling conditions were assumed. One of the graphs had Weyl asymptotics, while the second graph had a balanced vertex (in our case, it connected two internal and two external edges), and hence it was non-Weyl. Two experimental realizations of both graphs were studied. The obtained number of resonances nicely corresponded to theoretical predictions. In the first pair of networks, the Weyl network had 13 resonances in the given frequency range and the non-Weyl network had 11 resonances in this range. Both numbers were predicted theoretically. The second pair of networks was designed such that the edges emanating from the balanced vertex were longer than in the first pair of graphs, hence the difference between the Weyl and non-Weyl networks was more profound. The Weyl network had 15 resonances and the non-Weyl network had 12 resonances, as expected theoretically. The experiment shows that even if the Weyl formula is asymptotical, the theoretical formulæ for the number of resonances are reasonably satisfied even for ten to fifteen resonances.

Moreover, the paper theoretically explains why the constant by the leading term of the asymptotics is smaller for the non-Weyl graph. The main idea is that for the symmetric part of the wavefunction on both external edges the balanced vertex is transparent; in the given subspace the coupling condition is standard. Hence this part of the graph is equivalent to an internal edge connected by the standard condition to an external edge – hence there is no interaction between these two edges and the wave can move freely, effectively reducing the size of the graph.

To make the arguments more explicit, let us consider a vertex connecting two internal edges (with wavefunction components  $u_1$  and  $u_2$ ) and two external edges (with wavefunction components  $f_1$  and  $f_2$ ). Taking such parametrization that  $x = 0$  corresponds to this vertex for all the four edges, we get the coupling condition

$$u_1(0) = u_2(0) = f_1(0) = f_2(0), \quad u_1'(0) + u_2'(0) + f_1'(0) + f_2'(0) = 0. \quad (3.3)$$

Now we define symmetrization and antisymmetrization of these wavefunction components.

$$v_+ = \frac{1}{\sqrt{2}}(u_1 + u_2), \quad v_- = \frac{1}{\sqrt{2}}(u_1 - u_2), \quad g_+ = \frac{1}{\sqrt{2}}(f_1 + f_2), \quad g_- = \frac{1}{\sqrt{2}}(f_1 - f_2).$$

From (3.3) we have  $u_1(0) = u_2(0)$  and  $f_1(0) = f_2(0)$  and hence

$$\begin{aligned} v_+(0) &= \frac{1}{\sqrt{2}}(u_1(0) + u_2(0)) = \sqrt{2} u_1(0), \\ g_+(0) &= \frac{1}{\sqrt{2}}(f_1(0) + f_2(0)) = \sqrt{2} f_1(0), \\ v_-(0) &= \frac{1}{\sqrt{2}}(u_1(0) - u_2(0)) = \frac{1}{\sqrt{2}}(u_1(0) - u_1(0)) = 0, \\ g_-(0) &= \frac{1}{\sqrt{2}}(f_1(0) - f_2(0)) = \frac{1}{\sqrt{2}}(f_1(0) - f_1(0)) = 0. \end{aligned}$$

The coupling condition can be in the new functions written (using  $u_1(0) = f_1(0)$ ) as

$$v_+(0) = g_+(0), \quad v_+'(0) + g_+'(0) = 0, \quad v_-(0) = g_-(0) = 0. \quad (3.4)$$

Notice that the condition between the symmetric functions  $v_+$  and  $g_+$  is the standard condition connecting an internal and an external edge, while in the antisymmetric subspace we have the Dirichlet condition.

Let  $h$  be the wavefunction component on the rest of the graph. Then the map

$$\mathcal{U} : (u_1, u_2, f_1, f_2, h)^T \mapsto (v_+, v_-, g_+, g_-, h)^T \quad (3.5)$$

is unitary. It transforms the Hamiltonian  $H$  to the unitarily equivalent operator  $H_{\mathcal{U}} = \mathcal{U}H\mathcal{U}^{-1}$ . The “new” operator satisfies the coupling conditions (3.4). Therefore, one can replace the internal and external edge (formerly connected by the standard condition) by one external edge, reducing the internal part of the graph and making the graph non-Weyl.

### 3.2.2 Application of Topological Resonances in Experimental Investigation of a Fermi Golden Rule in Microwave Networks

In the paper [LLBS21] in the Appendix G, the results of M. Lee and M. Zworski [LZ16] were experimentally verified. The so-called *topological resonances*, i.e. the resonances arising as perturbations of former eigenvalues, were investigated. The Fermi golden rule (see Section 2.7) was verified in two particular examples of microwave networks.

There were phase shifters installed in the microwave network. These phase shifters allow to effectively change the lengths of the graph's edges. From the dependence of the absolute value of the scattering matrix determinant on the frequency, the position of the topological resonance was determined for each value of the optical length of the edges. Therefore, points on the resonance trajectory depending on the parameter  $t$  connected to the edge lengths were obtained. Using these points, the trajectory of the resonance in the complex plane was approximated by a parabola near the eigenvalue. As the final step, the second derivative of the imaginary part of the resonance with respect to the parameter  $t$  was found. The imaginary part of the momentum was fitted by the formula  $\text{Im } k = at^2 + b$ . The experimental values of the parameter  $a$  for both networks,  $a_{\text{exp}} = (-2.11 \pm 0.40) \text{ m}^{-1}$  and  $a_{\text{exp}} = (-0.46 \pm 0.03) \text{ m}^{-1}$ , are in good correspondence with the theoretical values  $a_{\text{th}} = -2.45 \text{ m}^{-1}$  and  $a_{\text{th}} = -0.46 \text{ m}^{-1}$ , respectively.

# Chapter 4

## Damped Wave Equation

One can equip the graph (in this chapter we will assume a finite graph with  $N$  internal edges) also with other operators than the Schrödinger operator. One of the simplest models how to describe a graph composed of vibrating strings is the system of equations

$$\partial_{tt}w_j(t, x) + 2a_j(x)\partial_t w_j(t, x) = \partial_{xx}w_j(t, x) + b(x)w_j(t, x), \quad (4.1)$$

where  $x$  denotes the space variable and  $t$  denotes the time. The functions  $a_j(x)$  are called the damping and the functions  $b_j(x)$  are denoted as potentials. The index  $j$  distinguishes the edge of the graph. The system of equations (4.1) is the system of partial differential equations which must be equipped with suitable initial and boundary conditions.

The system of equations (4.1) can be rewritten more elegantly as

$$\partial_t \begin{pmatrix} \vec{w}_0(t, x) \\ \vec{w}_1(t, x) \end{pmatrix} = \begin{pmatrix} 0 & I \\ I \frac{d^2}{dx^2} + B & -2A \end{pmatrix} \begin{pmatrix} \vec{w}_0(t, x) \\ \vec{w}_1(t, x) \end{pmatrix}. \quad (4.2)$$

Here,  $I$  is the  $N \times N$  identity matrix,  $A$  and  $B$  are diagonal  $N \times N$  matrices with entries  $a_j$  and  $b_j$ , respectively,  $\vec{w}_0$  is the vector of functions  $w_j$  and  $\vec{w}_1$  the vector of their time derivatives. The form (4.2) allows to easily solve the time dependence of the solution; it can be written as  $w_j(t, x) = e^{\lambda t}u_j(x)$ , where  $u_j(x)$  satisfies

$$\partial_{xx}u_j(x) - (\lambda^2 + 2\lambda a_j(x) - b_j(x))u_j(x) = 0.$$

The problem (4.1) can thus be reformulated as the eigenvalue problem for the operator

$$R = \begin{pmatrix} 0 & I \\ I \frac{d^2}{dx^2} + B & -2A \end{pmatrix},$$

with the domain consisting of two-component functions  $(\psi_1(x), \psi_2(x))^T$  with  $\psi_1, \psi_2 \in W^{2,2}(e_j)$  for the corresponding edge and satisfying the coupling conditions (2.2) at the vertices, where  $\Psi_j$  and  $\Psi'_j$  are the vectors of limits of the function values and derivatives at the vertices for the function  $\psi_1(x)$  and  $U_j$  the

coupling matrices. This coupling condition assures that the operator  $iR$  is self-adjoint for the case without damping  $A = 0$ .

The above-defined operator is, of course, non-selfadjoint. Its eigenvalues are typically approaching vertical lines in the complex plane as  $\lambda$  approaches complex infinity. The damped wave equation was intensively studied in the case of an interval, see, e.g. [CFNS91, CZ94, BF09, GH11]. For the studies of the wave equation on the graph we refer to the review [Zua13] and the references therein, where mostly controllability and observability of the problem are studied. Wave equation with the indefinite sign damping on a star graph was researched in [AMN13].

## 4.1 Results on the Damped Wave Equation

### 4.1.1 Eigenvalue Asymptotics for the Damped Wave Equation on Metric Graphs

The paper [FL17] in Appendix H is the first study of the equation (4.1) on a metric graph in its full generality. The  $4N^2$ -parameter space of the coupling conditions given by the coupling matrix  $U$  in (2.3) was considered in this paper. Spectral properties of the model are analysed, with the emphasis on the asymptotic properties for a large imaginary part of  $\lambda$ .

First, the asymptotic expansion of the eigenvalues of the operator  $R$  for an equilateral graph (graph with the same lengths of the edges) was found. The following result [FL17, Thm. 3.1] generalizes the result of P. Freitas and D. Borisov in the case of an interval [BF09]. It shows that the eigenvalues approach the vertical lines in the complex plane of  $\lambda$ , as the imaginary part of  $\lambda$  goes to infinity.

**Theorem 4.1.** *Consider an equilateral graph with  $N$  edges of unit length with the coupling between vertices given by a matrix  $U$  as above. Denote the damping and potential on each edge by  $a_j$  and  $b_j$ , respectively, and assume  $a_j \in C^1([0, 1])$  and  $b_j \in C^0([0, 1])$ . Then there exists a positive real number  $K_0$  such that for  $K > K_0$  if  $\lambda = r + iK$  is an eigenvalue, then  $\lambda + 2\pi i + \mathcal{O}(1/K)$  is also an eigenvalue. Similarly, if  $\lambda = r - iK$  is an eigenvalue, then  $\lambda - 2\pi i + \mathcal{O}(1/K)$  is also an eigenvalue. This means that there exist sequences of eigenvalues  $\lambda_{ns}$  satisfying*

$$\lambda_{ns} = 2\pi in + c_0^{(s)} + \mathcal{O}\left(\frac{1}{n}\right) \quad (4.3)$$

as  $n$  goes to infinity.

To describe the above-mentioned behaviour, we defined the notion of a high-frequency abscissa [FL17, Def. 3.4].

**Definition 4.2.** *We say that  $\omega_0$  is a high-frequency abscissa of the operator  $R$  if there exists a sequence of eigenvalues of  $R$ , say  $\{\lambda_n\}_{n=1}^\infty$ , such that*

$$\lim_{n \rightarrow \infty} \operatorname{Im} \lambda_n = \pm\infty \text{ and } \lim_{n \rightarrow \infty} \operatorname{Re} \lambda_n = \omega_0.$$

The number of distinct high-frequency abscissas of  $H$  will be called its abscissa count  $\alpha_c$ .

The results on the positions of the real parts of the eigenvalues are given in [FL17, Thm. 4.1, Cor. 4.2], see the Appendix H. Using the pseudo-orbit expansion, the results on the number of distinct high-frequency abscissas are obtained [FL17, Thm. 6.4], both for general equilateral graphs and for so-called *bipartite* graphs. A graph is bipartite if it admits partition into two classes such that every edge ends in different classes. To state the main result, we define the measure  $\mu_\infty$  [FL17, Def. 6.1].

**Definition 4.3.** *Let  $I$  be an open interval in  $\mathbb{R}$  and  $T > 0$ . Then we define the probability distribution  $\mu_T(I)$  by*

$$\mu_T(I) = \frac{\#\{\lambda : \operatorname{Re} \lambda \in I, |\operatorname{Im} \lambda| < T\}}{\#\{\lambda : |\operatorname{Im} \lambda| < T\}}.$$

We define  $\mu_\infty(I)$  by  $\lim_{T \rightarrow \infty} \mu_T(I)$ .

**Theorem 4.4.** *Let  $\Gamma$  be an equilateral graph with  $N$  edges of length one, with coupling given by (2.3) and with damping and potential functions  $a_j(x) \in C^1[0, 1]$ ,  $b_j(x) \in C^0[0, 1]$ , possibly discontinuous at the vertices.*

- i) The measure  $\mu_\infty$  is atomic with atoms with measures given by  $\frac{m_i}{2N}$  with  $m_i$  being a positive integer. The number of atoms is at most  $2N$  and  $\sum_{i=1}^{\alpha_c} m_i = 2N$ .*
- ii) If the graph is bipartite with Robin coupling on the boundary and standard coupling otherwise, then all  $m_i$ 's are even.*
- iii) For a tree graph with Robin coupling on the boundary and standard coupling otherwise, having all vertices of odd degree, there always exists a damping for which the maximum possible number of  $N$  atoms allowed by i) and ii) is achieved.*

Numerical examples for particular graphs are given, including an example where the case of different edge lengths was studied.



# Chapter 5

## Polyharmonic Operator

The final chapter is devoted to the operator that uses derivatives of higher order. One of the considered operators is a  $n$ -th multiple of the Laplacian and acts as

$$P_n = (-1)^n \frac{d^{2n}}{dx^{2n}}.$$

The second operator is its generalization which acts as

$$H_n = (-1)^n \frac{d^{2n}}{dx^{2n}} + \sum_{j=0}^m q_j(x) \frac{d^j}{dx^j}.$$

with  $m$  either fixed or dependent on  $n$  such that  $m(n) \leq n$ .

We will consider the simplest metric graph – the interval  $(0, T)$ . Since both operators are of the  $2n$ -th order, we prescribe  $n$  boundary conditions at each endpoint. We will use here the most common, Dirichlet boundary conditions

$$f^{(j)}(0) = f^{(j)}(T) = 0, \quad j = 0, \dots, n-1.$$

Polyharmonic operators have applications in the problems in linear elasticity theory (see, e.g. [BL13]). The polyharmonic operators have been recently studied, e.g. in [Kar21, KN22, BLPS21, RS21].

### 5.1 Spectral Determinant

One of the spectral quantities that could be studied for an operator is the spectral determinant. In [FL20], we investigated it for the polyharmonic operator. The spectral determinant is a generalization of the notion of the determinant of a matrix and tries to find the product of the eigenvalues for an operator which has (in general infinitely many) eigenvalues and no absolutely continuous spectrum. To define it, we first introduce the spectral zeta function for the operator  $\mathcal{T}$

$$\zeta_{\mathcal{T}}(s) = \sum_{j=1}^{\infty} \lambda_j^{-s},$$

where  $\lambda_j$  are the (non-zero) eigenvalues of  $\mathcal{T}$  and  $s$  is the complex parameter. If the operator has eigenvalues equal to zero, we remove them. The sum in the zeta function is typically convergent only for  $\text{Re } s$  larger than some positive value. However, one can meromorphically continue it to the whole complex plane. This allows to define the spectral determinant as

$$\det \mathcal{T} = \exp(-\zeta'_{\mathcal{T}}(0)).$$

This definition is in good correspondence with the usual definition of the determinant of a matrix, i.e. the product of the eigenvalues. If the operator  $\mathcal{T}$  has finitely many eigenvalues (for instance,  $O$ ), one can write

$$\zeta'_{\mathcal{T}}(0) = \sum_{j=1}^O \frac{\partial}{\partial s} \exp(-s \ln(\lambda_j))|_{s=0} = - \sum_{j=1}^O \ln(\lambda_j)$$

and hence

$$\det \mathcal{T} = \exp\left(\sum_{j=1}^O \ln(\lambda_j)\right) = \prod_{n=1}^O \lambda_j.$$

Spectral determinants have several applications in physics, for instance, string theory or quantum field theory [Dun08]. There are results on spectral determinants for Sturm-Liouville operators [LS77, GK19, ACF20], and Dirichlet Laplacians on balls or polygons [BGKE96, AS94]. A general result for elliptic operators [BFK95] was applied in [FL19, FL20].

## 5.2 Results on the Polyharmonic Operator

### 5.2.1 The Determinant of One-Dimensional Polyharmonic Operators of Arbitrary Order

The paper [FL20] in Appendix I studies the spectral determinant for the polyharmonic operator. Using the result on general elliptic operators [BFK95], it finds a closed expression for the spectral determinant of the polyharmonic operator  $P_n$ . Moreover, asymptotic expressions for large  $n$  are found for both operators. We copy here the results in [FL20, Thm. A, Thm. B].

**Theorem 5.1.** *The determinant of the polyharmonic operator  $P_n$  defined on the interval  $(0, T)$  with Dirichlet boundary conditions is given by*

$$\det P_n = \left(\frac{T}{2}\right)^{n^2} \frac{(4n)^n}{\prod_{k=1}^{n-1} [\sin^{2(n-k)}(\frac{k\pi}{2n})]} \prod_{k=0}^{n-1} \frac{k!}{(n+k)!}.$$

Furthermore, for large values of  $n$  it satisfies

$$\log(\det P_n) = -n^2 \log n + \left[ \frac{7\zeta(3)}{2\pi^2} + \frac{3}{2} + \log \frac{T}{4} \right] n^2 + \mathcal{O}(n), \quad (5.1)$$

where  $\zeta$  denotes the Riemann zeta function.

**Theorem 5.2.** *Let  $H_n$  be the polyharmonic operator defined on the interval  $(0, T)$  together with Dirichlet boundary conditions defined above, where  $q_j \in C^\infty([0, T])$  are complex functions defined on the interval  $[0, T]$ , and  $m$  is either fixed or dependent on  $n$  such that  $m(n) \leq n$ . Then, the determinant of the operator  $H_n$  satisfies*

$$\log(\det H_n) = \log(\det P_n) + \mathcal{O}(1/n) .$$

*as  $n$  goes to  $\infty$ . In particular, it has the same asymptotic behaviour as that of  $\log(\det P_n)$  given in (5.1).*

# Bibliography

- [AC71] AGUILAR, J. AND COMBES, J.-M. A class of analytic perturbations for one-body Schrödinger operators. *Commun. Math. Phys.*, 1971. vol. 22, pp. 269–279.
- [ACD<sup>+</sup>00] AKKERMANS, E., COMTET, A., DESBOIS, J., MONTAMBAUX, G., AND TEXIER, C. Spectral determinant on quantum graphs. *Ann. Phys.*, 2000. vol. 284, pp. 10–51.
- [ACF20] ALDANA, C., CAILLAU, J.-B., AND FREITAS, P. Maximal determinants of Schrödinger operators on bounded intervals. *J. Éc. polytech. Math.*, 2020. vol. 7, pp. 803–829.
- [AGB<sup>+</sup>14] ALLGAIER, M., GEHLER, S., BARKHOFEN, S., STÖCKMANN, H.-J., AND KUHL, U. Spectral properties of microwave graphs with local absorption. *Phys. Rev. E*, 2014. vol. 89, p. 022925.
- [AMN13] ABDALLAH, F., MERCIER, D., AND NICAISE, S. Exponential stability of the wave equation on a star shaped network within definite sign damping. *Palest. J. Math.*, 2013. vol. 2, pp. 113–143.
- [AS94] AURELL, E. AND SALOMONSON, P. On functional determinants of Laplacians in polygons and simplicial complexes. *Commun. Math. Phys.*, 1994. vol. 165, pp. 233–259.
- [BBK01] BERKOLAIKO, G., BOGOMOLNY, E., AND KEATING, J. Star graphs and Šeba billiards. *J. Phys. A: Math. Gen.*, 2001. vol. 34, pp. 335–350.
- [BC71] BASLEV, E. AND COMBES, J.-M. Spectral properties of many body Schrödinger operators with dilation analytic interactions. *Commun. Math. Phys.*, 1971. vol. 22, pp. 280–294.
- [BF09] BORISOV, D. AND FREITAS, P. Eigenvalue asymptotics, inverse problems and a trace formula for the linear damped wave equation. *J. Diff. Eq.*, 2009. vol. 247, pp. 3028–3039.
- [BFK95] BURGHELEA, D., FRIEDLANDER, L., AND KAPPELER, T. On the determinant of elliptic boundary value problems on a line segment. *Proc. Amer. Math. Soc.*, 1995. vol. 123, p. 3027.

## BIBLIOGRAPHY

---

- [BGKE96] BORDAG, M., GEYER, B., KIRSTEN, K., AND ELIZALDE, E. Zeta function determinant of the Laplace operator on the  $D$ -dimensional ball. *Commun. Math. Phys.*, 1996. vol. 179, pp. 215–234.
- [BHJ12] BAND, R., HARRISON, J. M., AND JOYNER, C. H. Finite pseudo orbit expansions for spectral quantities of quantum graphs. *J. Phys. A: Math. Theor.*, 2012. vol. 45, p. 325204.
- [BK13] BERKOLAIKO, G. AND KUCHMENT, P. *Introduction to Quantum Graphs*, vol. 186 of *Mathematical Surveys and Monographs*. AMS, 2013. ISBN 978-0-8218-9211-4.
- [BL13] BUOSO, D. AND LAMBERTI, P. D. Eigenvalues of polyharmonic operators on variable domains. *ESAIM Control Optim. Calc. Var.*, 2013. vol. 19, pp. 1225–1235.
- [BLPS21] BUOSO, D., LUZZINI, P., PROVENZANO, L., AND STUBBE, J. On the spectral asymptotics for the buckling problem. *J. Math. Phys.*, 2021. vol. 62, p. 121501.
- [Car12] CARLSON, R. Eigenvalue cluster traces for quantum graphs with equal edge lengths. *Rocky Mountain. J. Math.*, 2012. vol. 42, pp. 467–490.
- [CET10] CHEON, T., EXNER, P., AND TUREK, O. Approximation of a general singular vertex coupling in quantum graphs. *Ann. Phys.*, 2010. vol. 325, pp. 548–578.
- [CFNS91] CHEN, G., FULLING, S., NARCOWICH, F., AND SUN, S. Exponential decay of energy of evolution equations with locally distributed damping. *SIAM J. Appl. Math.*, 1991. vol. 51, pp. 266–301.
- [CZ94] COX, S. AND ZUAZUA, E. The rate at which energy decays in a damped string. *Commun. Partial Differ. Equ.*, 1994. vol. 19, pp. 213–243.
- [DEL10] DAVIES, E. B., EXNER, P., AND LIPOVSKÝ, J. Non-Weyl asymptotics for quantum graphs with general coupling conditions. *J. Phys. A: Math. Theor.*, 2010. vol. 43, p. 474013.
- [DP11] DAVIES, E. B. AND PUSHNITSKI, A. Non-Weyl resonance asymptotics for quantum graphs. *Analysis and PDE*, 2011. vol. 4, pp. 729–756.
- [Dun08] DUNNE, G. V. Functional determinants in quantum field theory. *J. Phys. A: Math. Theor.*, 2008. vol. 41, p. 304006.
- [EK15] EXNER, P. AND KOVAŘÍK, H. *Quantum Waveguides*. Springer International, Heiderberg, 2015. ISBN 978-3-319-18575-0.

## BIBLIOGRAPHY

---

- [EL07] EXNER, P. AND LIPOVSKÝ, J. Equivalence of resolvent and scattering resonances on quantum graphs. In *Adventures in Mathematical Physics (Proceedings, Cergy-Pontoise 2006)*, vol. 447. Providence, R.I., 2007 pp. 73–81.
- [EL10] EXNER, P. AND LIPOVSKÝ, J. Resonances from perturbations of quantum graphs with rationally related edges. *J. Phys. A: Math. Theor.*, 2010. vol. 43, p. 1053.
- [EL11] EXNER, P. AND LIPOVSKÝ, J. Non-Weyl resonance asymptotics for quantum graphs in a magnetic field. *Phys. Lett. A*, 2011. vol. 375, pp. 805–807.
- [EL17] EXNER, P. AND LIPOVSKÝ, J. Pseudo-orbit approach to trajectories of resonances in quantum graphs with general vertex coupling: Fermi rule and high-energy asymptotics. *J. Math. Phys.*, 2017. vol. 58, p. 042101.
- [EL19] EXNER, P. AND LIPOVSKÝ, J. Spectral asymptotics of the Laplacian on Platonic solids graphs. *J. Math. Phys.*, 2019. vol. 60, p. 122101.
- [EL20] EXNER, P. AND LIPOVSKÝ, J. Topological bulk-edge effects in quantum graph transport. *Phys. Lett. A*, 2020. vol. 384, p. 126390.
- [ET18] EXNER, P. AND TATER, M. Quantum graphs with vertices of a preferred orientation. *Phys. Lett. A*, 2018. vol. 382, pp. 283–287.
- [Eva98] EVANS, L. C. *Partial Differential Equations*. Providence, R.I.: American Mathematical Society, 1998. ISBN 9780821849743.
- [Exn07] EXNER, P. Leaky quantum graphs: A review. In *Analysis on Graphs and Applications*, vol. 77 of *Proceedings of Symposia in Pure Mathematics*. 2007 pp. 523–564.
- [FL17] FREITAS, P. AND LIPOVSKÝ, J. Eigenvalue asymptotics for the damped wave equation on metric graphs. *J. Diff. Eq.*, 2017. vol. 263, pp. 2780–2811.
- [FL19] FREITAS, P. AND LIPOVSKÝ, J. Spectral determinant for the damped wave equation on an interval. *Acta Physica Polonica A*, 2019. vol. 136, pp. 817–823.
- [FL20] FREITAS, P. AND LIPOVSKÝ, J. The determinant of one-dimensional polyharmonic operators of arbitrary order. *J. Funct. Anal.*, 2020. vol. 279, p. 108783.
- [FL21] FREITAS, P. AND LIPOVSKÝ, J. A Gelfand-Levitan trace formula for generic quantum graphs. *Anal. Math. Phys.*, 2021. vol. 11, p. 56.

## BIBLIOGRAPHY

---

- [FT00] FÜLÖP, T. AND TSUTSUI, I. A free particle on a circle with point interaction. *Phys. Lett. A*, 2000. vol. 264, pp. 366–374.
- [GH11] GESZTESY, F. AND HOLDEN, H. The damped string problem revisited. *J. Diff. Eq.*, 2011. vol. 251, pp. 1086–1127.
- [GK19] GESZTESY, F. AND KIRSTEN, K. Effective computation of traces, determinants, and  $\zeta$ -functions for Sturm-Liouville operators. *J. Funct. Anal.*, 2019. vol. 276, pp. 520–562.
- [GL53] GEL’FAND, I. M. AND LEVITAN, B. M. On a simple identity for the characteristic values of a differential operator of the second order. *Doklady Akad. Nauk SSSR (Russian)*, 1953. vol. 88, pp. 593–596.
- [GS01] GUTKIN, B. AND SMILANSKY, U. Can one hear the shape of a graph? *J. Phys. A: Math. Gen.*, 2001. vol. 34, pp. 6061–6068.
- [Har00] HARMER, M. Hermitian symplectic geometry and extension theory. *J. Phys. A: Math. Gen.*, 2000. vol. 33, pp. 9193–9203.
- [HBP<sup>+</sup>04] HUL, O., BAUCH, S., PAKOŃSKI, P., SAVYTSKYI, N., AND ŻYCKOWSKI, K. Experimental simulation of quantum graphs by microwave networks. *Phys. Rev. E*, 2004. vol. 69, p. 056205.
- [HK60] HALBERG, C. J. A. AND KRAMER, V. A. A generalization of the trace concept. *Duke Math. J.*, 1960. vol. 27, pp. 607–617.
- [HŁB<sup>+</sup>12] HUL, O., ŁAWNICZAK, M., BAUCH, S., SAWICKI, A., KUŚ, M., AND SIRKO, L. Are scattering properties of graphs uniquely connected to their shapes? *Phys. Rev. Lett.*, 2012. vol. 109, p. 040402.
- [Ing22a] INGREMEAU, M. Scattering resonances of large weakly open quantum graphs. *Pure Appl. Anal.*, 2022. vol. 4, pp. 49–83.
- [Ing22b] INGREMEAU, M. A trace formula for scattering resonances of unbalanced quantum graphs, 2022. ArXiv preprint, arXiv:2206.12460.
- [Ivr80] IVRII, V. J. The second term of the spectral asymptotics for a Laplace–Beltrami operator on manifolds with boundary. *Funktsional. Anal. i Prilozhen*, 1980. vol. 14, no. 3, pp. 25–34.
- [Ivr16] IVRII, V. 100 years of Weyl’s law. *Bull. Math. Sci.*, 2016. vol. 6, pp. 379–452.
- [Kar21] KARACHIK, V. Dirichlet and Neumann boundary value problems for the polyharmonic equation in the unit ball. *Mathematics*, 2021. vol. 9, p. 1907.

## BIBLIOGRAPHY

---

- [KN22] KESSEBÖHMER, M. AND NIEMANN, A. Approximation order of Kolmogorov diameters via Lq-spectra and applications to polyharmonic operators. *J. Funct. Anal.*, 2022. vol. 283, p. 109598.
- [KS97] KOTTOS, T. AND SMILANSKY, U. Quantum chaos on graphs. *Phys. Rev. Lett.*, 1997. vol. 79, pp. 4794–4797.
- [KS99a] KOSTRYKIN, V. AND SCHRADER, R. Kirchhoff’s rule for quantum wires. *J. Phys. A: Math. Gen*, 1999. vol. 32, no. 4, pp. 595–630.
- [KS99b] KOTTOS, T. AND SMILANSKY, U. Periodic orbit theory and spectral statistics for quantum graphs. *Ann. Phys.*, 1999. vol. 274, pp. 76–124.
- [KS00] KOTTOS, T. AND SMILANSKY, U. Chaotic scattering on graphs. *Phys. Rev. Lett.*, 2000. vol. 85, pp. 968–971.
- [KS18] KURASOV, P. AND SUHR, R. Schrödinger operators on graphs and geometry. III. General vertex conditions and counterexamples. *J. Math. Phys.*, 2018. vol. 59, p. 102104.
- [Kuc08] KUCHMENT, P. Quantum graphs: An introduction and a brief survey. In *Analysis on Graphs and its Applications*, Proc. Symp. Pure. Math. AMS, 2008 pp. 291–314.
- [Lip15] LIPOVSKÝ, J. Pseudo-orbit expansion for the resonance condition on quantum graphs and the resonance asymptotics. *Acta Physica Polonica A*, 2015. vol. 128, pp. 968–973.
- [Lip16a] LIPOVSKÝ, J. On the effective size of a non-Weyl graph. *J. Phys. A: Math. Theor.*, 2016. vol. 49, p. 375202.
- [Lip16b] LIPOVSKÝ, J. Quantum graphs and their resonance properties. *Acta Physica Slovaca*, 2016. vol. 66, no. 4, pp. 265–363.
- [ŁKB<sup>+</sup>21] ŁAWNICZAK, M., KURASOV, P., BAUCH, S., BIAŁOUS, M., AKHSHANI, A., AND SIRKO, L. A new spectral invariant for quantum graphs. *Sci. Rep.*, 2021. vol. 11, p. 15342.
- [ŁLBS21] ŁAWNICZAK, M., LIPOVSKÝ, J., BIAŁOUS, M., AND SIRKO, L. Application of topological resonances in experimental investigation of a Fermi golden rule in microwave networks. *Phys. Rev. E*, 2021. vol. 103, p. 032208.
- [ŁLS19] ŁAWNICZAK, M., LIPOVSKÝ, J., AND SIRKO, L. Non-Weyl microwave graphs. *Phys. Rev. Lett.*, 2019. vol. 122, p. 140503.
- [Lor10] LORENTZ, H. Alte und neue Fragen der Physik. *Physikal. Zeitschr.*, 1910. vol. 11, pp. 1234–1257.



## BIBLIOGRAPHY

---

- [LS77] LEVIT, S. AND SMILANSKY, U. A theorem of infinite products of eigenvalues of Sturm-Liouville type operators. *Proc. Am. Math. Soc.*, 1977. vol. 65, pp. 299–302.
- [ŁSB<sup>+</sup>14] ŁAWNICZAK, M., SAWICKI, A., BAUCH, S., KUŚ, M., AND SIRKO, L. Resonances and poles in isoscattering microwave networks and graphs. *Phys. Rev. E*, 2014. vol. 89, p. 032911.
- [LZ16] LEE, M. AND ZWORSKI, M. A Fermi golden rule for quantum graphs. *J. Math. Phys.*, 2016. vol. 57, p. 092101.
- [Pau36] PAULING, L. The diamagnetic anisotropy of aromatic molecules. *J. Chem. Phys.*, 1936. vol. 4, pp. 673–677.
- [Pos12] POST, O. *Spectral Analysis on Graph-like Spaces*. Springer, Heidelberg, Heidelberg, 2012. ISBN 978-3-642-23839-0.
- [RAJ<sup>+</sup>16] REHEMANJIANG, A., ALLGAIER, M., JOYNER, C. H., MÜLLER, S., SIEBER, M., KUHL, U., AND STÖCKMANN, H.-J. Microwave realization of the Gaussian symplectic ensemble. *Phys. Rev. Lett.*, 2016. vol. 117, p. 064101.
- [Rot83] ROTH, J.-P. Spectre du Laplacien sur un graphe. *C.R. Acad. Sci. Paris*, 1983. vol. 296, pp. 793–795.
- [RS53] RUEDENBERG, K. AND SCHERR, C. Free-electron network model for conjugated systems, I. Theory. *J. Chem. Phys.*, 1953. vol. 21, pp. 1565–1581.
- [RS78] REED, M. AND SIMON, B. *Methods of Modern Mathematical Physics, Vol. IV: Analysis of Operators*. Academic Press, 1978. ISBN 978-0125850049.
- [RS21] ROZENBLUM, G. V. AND SHARGORODSKY, E. M. Eigenvalue asymptotics for weighted polyharmonic operator with a singular measure in the critical case. *Funct. Anal. Appl.*, 2021. vol. 55, pp. 170–173.
- [Som10] SOMMERFELD, A. Die Greensche Funktion der Schwingungsgleichung für ein beliebiges Gebiet. *Physikal. Zeitschr.*, 1910. vol. 11, pp. 1057–1066.
- [Wey11] WEYL, H. Über die asymptotische Verteilung der Eigenwerte. *Nachrichten von der Gesellschaft der Wissenschaften zu Göttingen, Mathematisch-Physikalische Klasse*, 1911. vol. 2, pp. 110–117.
- [Yan13] YANG, C.-F. Regularized trace for Sturm-Liouville differential operator on a star-shaped graph. *Complex Anal. Oper. Theory*, 2013. vol. 7, pp. 1185–1196.

## BIBLIOGRAPHY

---

- [Yan14] YANG, C.-F. Traces of Sturm-Liouville operators with discontinuities. *Inverse Probl. Sci. Eng.*, 2014. vol. 22, pp. 803–813.
- [YY07] YANG, C.-F. AND YANG, J.-X. Large eigenvalues and traces of Sturm-Liouville equations on star-shaped graphs. *Methods Appl. Anal.*, 2007. vol. 14, pp. 179–196.
- [Zua13] ZUAZUA, E. Control and stabilization of waves on 1-d networks. In *Modelling and Optimisation of Flows on Networks, in: Lecture Notes in Math., CIME Subseries*, vol. 2062. Springer Verlag, 2013 pp. 463–493.

# List of Notation

$A$	diagonal matrix with entries $a_j$
$a_j$	damping components
$B$	diagonal matrix with entries $b_j$
$b_j$	potential components
$C^j$	the space of functions with their $j$ -th derivatives continuous
$C^\infty$	the space of bounded functions
$c$	velocity of light
$\Gamma$	metric graph
$\gamma$	periodic orbit
$\tilde{\gamma}$	pseudo-orbit
$\bar{\gamma}$	irreducible pseudo-orbit
$d_j$	degree of the vertex
$E, \lambda_n$	energy, eigenvalue of $H$
$\mathcal{E}_i$	the set of internal edges of a graph
$\mathcal{E}_e$	the set of external edges of a graph
$e^s$	generalized eigenfunction
$\varepsilon$	dielectric constant
$H$	Hamiltonian
$H_\theta$	Hamiltonian after complex scaling
$\mathcal{H}$	Hilbert space
$H_n, P_n$	polyharmonic operators
$I, I_n$	identity matrix
$J$	matrix with all entries equal to one
$k$	square root of energy, the momentum
$\dot{k}, \ddot{k}$	first and second derivative of $k$ with respect to $t$
$\ell_j, T$	edge length
$L$	matrix $\text{diag}(\ell_1, \dots, \ell_N, \ell_1, \dots, \ell_N)$
$M$	number of external edges
$\mu_n$	sequence of zeros of $\prod_{i=1}^N (-k \sin k\ell_i)$
$\mu_T, \mu_\infty$	measures used for the damped wave equation
$N$	number of internal edges
$N(\lambda)$	counting function
$q$	electric potential
$\bar{q}$	average of the potential

LIST OF NOTATION

---

$\psi, f, g, h, u, v$	elements of the Hilbert space, wavefunction (component)
$\Psi_j, \Psi$	vector of limits of the function values at the vertex
$\Psi'_j, \Psi'$	vector of limits of the outgoing derivatives at the vertex
$U_j, U, A_j, B_j$	coupling matrices
$U_\theta$	complex scaling operator
$\mathcal{U}$	unitary map
$U_{ij}$	potential difference between the conductors
$\tilde{U}$	effective coupling matrix
$Q$	the matrix $\begin{pmatrix} 0 & I_N \\ I_N & 0 \end{pmatrix}$
$R$	operator for the damped wave equation
$S(k)$	scattering matrix
$\tilde{\sigma}$	effective vertex scattering matrix
$\sigma$	spectrum
$\sigma_{\text{pp}}$	pure point spectrum
$\tilde{\Sigma}$	matrix similar to the block diagonal matrix with blocks $\tilde{\sigma}$
$t$	parameter giving the edge lengths
$V$	sum of the lengths of the internal edges of a graph
$\mathcal{V}$	set of vertices
$\tilde{V}$	number of vertices of a graph
$W$	effective size of a graph
$W^{2,2}, W^{1,1}$	Sobolev spaces
$w_j(t, x)$	time-dependent wavefunction for the damped wave equation
$\mathcal{X}_j, \mathcal{X}, v$	particular vertex of a graph
$\zeta$	the Riemann zeta function
$\zeta_{\mathcal{T}}$	spectral zeta function for the operator $\mathcal{T}$
$\Omega$	bounded domain in $\mathbb{R}^d$
$\omega_d$	volume of the unit ball in $d$ dimensions
$\omega$	angular frequency
$\partial\Omega$	boundary of the domain $\Omega$
$\partial$	partial derivative

# Attachments

# Appendix A

## Spectral Asymptotics of the Laplacian on Platonic Solids Graphs

Published in: P. Exner, J. Lipovský, Spectral asymptotics of the Laplacian on Platonic solids graphs, *J. Math. Phys.* **60** (2019), 122101

<https://doi.org/10.1063/1.5116100>

Preprints: arXiv: 1906.09091 [math.sp]

mp\_arc: 19-42

# Appendix B

## Topological Bulk-Edge Effects in Quantum Graph Transport

Published in: P. Exner, J. Lipovský, Topological bulk-edge effects in quantum graph transport, *Phys. Lett. A* **384** (2020), 126390.

<https://doi.org/10.1016/j.physleta.2020.126390>

Preprints: arXiv: 2001.10735 [math-ph]

mp\_arc: 20-5

# Appendix C

## A Gelfand-Levitan Trace Formula for Generic Quantum Graphs

Published in: P. Freitas, J. Lipovský, A Gelfand-Levitan trace formula for generic quantum graphs, *Anal. Math. Phys.* **11** (2021), 56.

<https://doi.org/10.1007/s13324-021-00487-3>

Preprints: arXiv: 1901.07790 [math-ph]

mp\_arc: 19-4



## Appendix D

# Pseudo-Orbit Approach to Trajectories of Resonances in Quantum Graphs with General Vertex Coupling: Fermi Rule and High-Energy Asymptotics

Published in: P. Exner, J. Lipovský, Pseudo-orbit approach to trajectories of resonances in quantum graphs with general vertex coupling: Fermi rule and high-energy asymptotics, *J. Math. Phys.* **58** (2017), 042101.

<http://dx.doi.org/10.1063/1.4979048>

Preprints: arXiv: 1608.03978 [math-ph]

mp\_arc: 16-67

# Appendix E

## On the Effective Size of a Non-Weyl Graph

Published in: J. Lipovský, On the effective size of a non-Weyl graph, *J. Phys. A: Math. Theor.* **49** (2016), 375202.

<http://dx.doi.org/10.1088/1751-8113/49/37/375202>

Preprints: arXiv: 1507.04176 [math-ph]

mp\_arc: 15-65

# Appendix F

## Non-Weyl Microwave Graphs

Published in: M. Ławniczak, J. Lipovský, and L. Sirko, Non-Weyl microwave graphs, *Phys. Rev. Lett.* **122** (2019), 140503.

<https://doi.org/10.1103/PhysRevLett.122.140503>

Preprint: arXiv: 1904.06905 [quant-ph]

# Appendix G

## Application of Topological Resonances in Experimental Investigation of a Fermi Golden Rule in Microwave Networks

Published in: M. Ławniczak, J. Lipovský, M. Białous, L. Sirko, Application of topological resonances in experimental investigation of a Fermi golden rule in microwave networks, *Phys. Rev. E* **103** (2021), 032208.

<https://doi.org/10.1103/PhysRevE.103.032208>

Preprint: arXiv: 2108.05584 [quant-ph]

# Appendix H

## Eigenvalue Asymptotics for the Damped Wave Equation on Metric Graphs

Published in: P. Freitas, J. Lipovský, Eigenvalue asymptotics for the damped wave equation on metric graphs, *J. Diff. Eq.* **263** (2017), 2780–2811.

<http://dx.doi.org/10.1016/j.jde.2017.04.012>

Preprint: arXiv: 1307.6377 [math-ph]

# Appendix I

## The Determinant of One-Dimensional Polyharmonic Operators of Arbitrary Order

Published in: P. Freitas, J. Lipovský, The determinant of one-dimensional polyharmonic operators of arbitrary order, *J. Funct. Anal.* **279** (2020), 108783.

<https://doi.org/10.1016/j.jfa.2020.108783>

Preprint: arXiv: 2001.04703 [math-ph]